# Braking Availability Tester (BAT) for Winter Runway

by

Kamal Joshi

A thesis
presented to the University of Waterloo
in fulfillment of the
thesis requirement for the degree of
Master of Applied Science
in
Mechanical Engineering

Waterloo, Ontario, Canada, 2013

I hereby declare that I am the sole author of this thesis. This is a true copy of the thesis, including any required final revisions, as accepted by my examiners.

I understand that my thesis may be made electronically available to the public.

## Abstract

This thesis is concerned with the development of a new measurement device for the realistic assessment of braking capability of landing airplanes for winter runways. Landing represents one of the most safety-critical phases of aircraft operation. Aircraft runway excursion incidents occur due to the unpredictability of the runway pavement condition. This is especially true during winter time when the runway is often covered by deformable contaminants. Several accidents are discussed that list the deteriorated condition of the runway pavement and the inability to accurately report this condition as the main causes for the excursions. The accuracy of the approaches currently adopted by the airport authorities around the world to monitor the condition of the runway pavement are evaluated.

The conventional and current practice of runway condition monitoring is focused on identifying the maximum tire-pavement frictional drag ($\mu$ value) and often neglect the characteristics of actual aircraft brake control system as well as the comprehensive effects coming from various factors such as deformable contaminants on the winter runway. The braking availability tester discussed here is designed to take a different approach for the realistic assessment of braking availability of landing aircrafts. The main idea of this device is to mimic the braking operation of actual aircrafts as closely as possible by incorporating the same brake mechanism and the brake control system used in existing aircrafts. The architecture of the device from the ground-up including the suite of sensors, the structure of the wheel, important actuators, and the real-time brake control system are discussed in detail. More importantly, the operational principles of the braking availability tester (BAT) are outlined which help one understand how the system works together.

A new method to quantify the braking availability on the runway using the BAT is explained. The testing and data collection strategy for implementing this technique is also outlined. Additionally, the results from preliminary tests are presented to verify the functionality of the BAT. The results are used to verify that the BAT operates with the brake control system of an aircraft. Finally, experimental data sets from dry and contaminated pavement testing are presented to show the effect of different weather conditions on the operation of the BAT.

**Acknowledgements**

I would like to sincerely thank my supervisor, Professor Soo Jeon, for his guidance, advice, and support during my journey as an MASc student. I can not thank him enough for his invaluable support. I am blessed to have an understanding, friendly, humble, and knowledgeable supervisor. Thank you for understanding every situation and providing me with your brilliant insights into every problem I faced.

I would like to thank my fellow office members Vahid, Hyunki, Olabanjo and Bonghun for sharing their point of view on various technical discussions.

I would like to acknowledge Team Eagle Ltd. and the Ontario Centers of Excellence (OCE) for the financial support for this project. I would like to thank the folks at Team Eagle Ltd. for providing me with the opportunity to contribute to this innovative BAT project. I would also like to thank Arnold Beck at the Meggit Aircraft Braking Systems Corp. for helping me understand aircraft brake control system and providing me with his knowledge on various aircraft related topics. I would like to thank Joe Breen and other members at the FAA for valuable discussions and sharing their approach of using the aircraft ABS for contaminated runways and the nose tire for instrumentation. I am truly grateful and privileged to have worked with a team of experienced and skilled professionals.

Mom and Dad, Thank you for teaching me respect and confidence. Thank you for acknowledging how hard I have worked, but also know that I would not be here without you. With your support, I plan on fulfilling all my goals in life.

## Dedication

I would like to dedicate this thesis to the people that have always supported me with my decisions in life. It is because of your support I am able to successfully complete my journey through Masters of Applied Sciences program at University of Waterloo.

Also, this thesis is dedicated to my family and friends that always believed in me and provided me with inspiration and motivation. Finally, I dedicate this thesis to all those who believe in the richness of learning.

# Table of Contents

# List of Tables

# List of Figures

# Chapter 1

# Introduction

This chapter discusses the importance of being able to quantify the braking availability on the runway for any particular aircraft. Firstly, some interesting statistical data and runway excursions are discussed to motivate research in this specific field. To motivate further, historical runway excursions are discussed briefly to breakdown the probable causes of each incident. More importantly, methods currently used to predict tire pavement interactions are discussed in detail along with the techniques used to observe the condition of the runway. After further analysis, comments are made about the inability of current techniques to estimate safe landing for aircrafts on contaminated runways.

## 1.1 Motivation

Between 1995 to 2008, 80% of the runway related accidents were landing excursions or veer-off. There have been 1013 accidents in North America since 1945, resulting in 13479 fatalities and 187 ground fatalities. Out of all the fatalities, Canada accounts for 1746 fatalities which make up 13% of deaths in North America due to an aircraft accident. Specifically, Canada is third on the list among twenty-five geographic locations having the highest number of airliner accidents averaging up to 10 deaths per incident [1]. For many aircraft accidents, weather is one of the main factors that pose safety hazard in the

form of high wind shear, contaminated runway, low visibility, icing, thunderstorm, lightning strike and heavy rainfall or snowfall. Geographically, being close to the North Pole, Canada receives extreme weather during the season of winter. Airport operations become more careful about any type of activity on the runway. Even though the runway is well maintained and kept clear under poor weather conditions during winter, the runway gets covered with various contaminants such as slush, ice and snow. For the aviation industry, such contaminants on the runway are potential safety threats since they can affect the performance of an aircraft during take-off and landing. More often than not, contaminants result in decreased tire-pavement friction, which greatly affects the performance of the aircraft during deceleration when coming to a stop after touch-down on the runway. Reportedly, the ineffective braking due to contaminated runway is one of the top risk factors among all runway excursion incidents [2]. This makes it crucial to report accurate information of the runway to the pilots in a timely manner [3, 4]. There are many aircraft accidents resulting from the airport operators inability to properly report the condition of the runway to the pilot. According to historical data from past 22 years, the risk of overrun is increased by 8 folds when there is standing water and slush on the runway [5]. Some of the accidents that list contaminated runway as a probable cause date back to half a century [1]. The famous Munich Air Disaster in 1958 [1] was the first major accident that identified the slush on the runway as the probable cause of runway excursion.

Similarly, the runway overrun in 1982 at the Boston-Logan International airport [6] showed lack of braking effectiveness on the ice-covered runway. This caused McDonnell Douglas DC 10 30CF to overrun the runway, resulting in two passenger fatalities and the airplane to be damaged beyond repair. Even though the ambient temperature was above freezing point at the time of the accident, snow covered pavement caused continued precipitation to change into ice on contact, forming a thin layer of ice. Additionally, analysis of the black box data regarding the deceleration from earlier aircraft landing showed effective braking coefficient of 0.08 or less for the length of the runway. This is close to 0.07, usually correlated with the effective braking coefficient of layer of smooth ice. It was noted that regardless of the aircraft crews performance, the ability to stop the aircraft on this slippery runway was marginal. Until the late 1990s, there were no quantitative measures provided for correlating actual runway condition with airplane stopping performance, measurement

of runway friction or minimum runway braking action conditions. Moreover, Federal Aviation Administration (FAA) at the time did not require the Aircraft Flight Manual (AFM) to contain any information regarding stopping performances on low friction coefficient surfaces. This did not allow the accident pilot to correlate the Braking Action Reports (BARs) with the data. More importantly, the BARs do not provide enough quantitative evidence to make decisions about operating on a slippery runway since it differs from one pilot to another. Pilots who land successfully report runway conditions and events specific to their aircraft and expertise. These reports do not apply to other aircrafts with different make and model that are operated by a different pilot under different conditions. The need for extending the minimum length of the runway for landing under ice and snow due to reduction in braking availability was one of the major recommendations to the Federal Aviation Regulations (FAR) after this incident. More importantly, the inadequacy of the airport operations to report the condition of the runway by measuring the slipperiness of the runway and the inability to correlate the braking ability on the contaminated runway with the aircraft stopping distance were overlooked.

One of more recent accidents in 2005 involves Boeing 737-7H4 [7], operated by Southwest Airlines (SWA), rolled out of the Chicago Midway airport and onto the adjacent road. On the day of the accident 25 cm of snow had accumulated and the runway was cleared 21 minutes before the accident. There were mixed BARs provided to the accident pilots. Air Traffic Control (ATC) reported "good" for the first half of the runway while "fair" for the second half.[1] Onboard Performance Computer (OPC) provided positive landing stopping distance of 560 feet for fair and 40 feet for poor conditions to the accident pilots after calculating the arrival landing distance, which was mainly due to the use of uncorrelated data. However, for both cases there was not enough training provided to SWA crew members to understand the assumptions that OPC was making for the dataset used. Calculations provided by OPC only considered tail wind of 5 knots and assumed timely application of the reveres thrust. For all landings, SWA pilots are required to use reverse thruster as soon as the nose wheels make contact with the pavement. The accident pilots were unaware of the fact and believed that using the reverse thrust would provide them with extra stopping distance. According to the Flight Data recorder (FDR) the thrust reversers were fully

[1]Table 1.1 and Table 1.2 explain the Good, Fair and Poor braking conditions in more detail.

deployed 18 seconds after touchdown. FDR data from aircrafts that landed successfully prior to the accident showed timely application of the reverse thrusters. In order to assess aircrafts lading performance capability, establishing a method to correlate aircrafts braking ability with runway surface condition was stressed upon during the accident investigation.

Another notable incident due to contaminated runway occurred on April 12 2007 at Traverse City in Michigan [8]. It was clear that aircrafts antiskid and braking systems were working to their maximum effectiveness and Cherry Capital Airport operations had provided snow removal services on timely manner to suffice FAR. The pilots failed to anticipate the lack of braking availability on the runway due to the accumulation of wet snow. The paraphrasing of BARs by Air Traffic Control (ATC) to the accident pilots was unclear which led them to believe that safe landing was possible. Accident pilots failed to reassess their approach in changing weather and runway condition, which led to the runway excursion .

## 1.2 Tire - Pavement Interaction

Many archives of data are available from flight testing over time to understand the aircraft tire-pavement interaction. These flight tests have been performed on smooth, hard-surface and dry runways considering control variables such as glide slopes, higher sink rates, maximum manual braking and a specific airplane weight to name a few. However, the data is not accurate for contaminated runway when extrapolated from these tests due to incompatibility of the testing environment. Besides, the results do not consider brake efficiency, runway surface condition, speed reducing equipments, tire condition and skills of the pilot. FAA requires airline operators to calculate pre-flight landing distance in order to assess the ability of the aircraft to take-off with the weight and land at the destination airport. However, calculations for arrival landing distance are not regulated by FAA. This allows the airline operators to pick the method they see fit, instead of following safety margins or FAA approved set of correlation data to evaluate the method. Additionally, use of data from various sources such as aircraft manufacturers, contractors or in-house personnel reduces accuracy of the result. The airline operators are not aware of all the assumptions

made related to the aircrafts ability to brake under certain pavement condition when using third-party data [7]. Software is used to provide landing distance under various conditions using the most corresponding flight test data. The runway operators multiply the final landing distance provided by the software by a factor to increase safety margin [3]. FAA has now made it mandatory for all airline operators to do landing distance assessment prior to approach and add 15% safety factor.

## 1.3 Runway Condition Reporting

Runway surface assessment has been one of the main concerns for National Transport Safety Board (NTSB) and FAA over past few decades. During the early 80s the large airplane operations on contaminated runways [9] encouraged the aviation industry to provide consistent and reliable methods to evaluate runway surface conditions. This is very difficult to achieve due to the nature of naturally occurring contaminants that continuously change conditions of the runway and countless different models of aircraft from various manufacturers. It also increases the complexity of the mathematical model that can be used for aircrafts [10]. To this date, no significant advances have been made to reduce the subjectivity and variances between reports. Despite many years of effort to standardize methods for reporting runway conditions, all the working groups have not reached a consensus. Moreover, there is no consistency in terminology in BARs or contaminant type and depth reports that can be recognized internationally. Most importantly, the correlation between the type and depth of the contaminants with the BARs is yet to be found [7]. Up to date there is no recognized or established standard way to relate the friction coefficient read by the Continuous Friction Measurement Equipment (CFME) or Decelerometer with the friction felt by the aircraft [3]. After Chicago Midway International incident, the NTSB decided to re-evaluate the three methods (Braking Action Reports, Runway Contaminant Type and Depth Observation, and Ground Surface Friction Measurement Devices) practiced to assess the runway pavement condition.

### 1.3.1 Braking Action Reports (BAR)

Braking Action Reports (BARs) are subjective to pilots experience, perception and expectations. If a fair BAR was reported to a pilot before landing, he or she might feel the same or completely different situation after landing successfully. The dependability on the type and model of the aircraft being used along with deceleration devices used to bring the aircraft to a stop could greatly influence the outcome of the BARs. This increases the variability of the BARs significantly between pilots even under dry and bare runway pavement. In 2006, FAA provided guidelines that outlined the conditions and the terminology to be used with the BARs outlined in table 1.1[2].

Table 1.1: Braking Action Report Terminology *(SAFO 06012 2006)*

| | |
|---|---|
| **Good** | More braking capability is available than is used in typical deceleration on a non-limiting runway (i.e., a runway with additional stopping distance available). However, the landing distance will be longer than the certified (un-factored) dry runway landing distance, even with a well-executed landing and maximum effort braking. |
| **Fair/Medium** | Noticeably degraded braking conditions. Expect and plan for a longer stopping distance such as might be expected on a packed or compacted snow-covered runway. |
| **Poor** | Very degraded braking conditions with a potential for hydroplaning. Expect and plan for a significantly longer stopping distance such as might be expected on an ice covered runway. |
| **Nil** | No braking action and poor directional control can be expected. |

For pilots to interpret BARs provided to them, SAFO 06012 also provided relationship between the BARs and runway surface condition as outlined in table 1.2. When these correlations are provided, pilots are still expected to use sound judgement to assess the

[2]Conditions specified as "nil" braking action are not considered safe, therefore operations under conditions specified as such should not be conducted. Do not attempt to operate on surfaces reported or expected to have nil braking action.

applicability of the information to their aircrafts landing performance[3]. However, after setting the terminology and their respective correlation the matter of subjectivity still remains. Moreover, many of the overrun incidents investigations in the past have shown that there were mixed BARs from pilots that successfully landed prior to the incident. More importantly, many times ground vehicle runway friction measurements conflict BARs. FAA still has not provided a standard procedure or a list of criteria that should be used to deliver or develop the BARs.

Table 1.2: BARs and Runway Surface Condition Relationship *(SAFO 06012 2006)*

| **Braking Action** | **Contaminant** |
|---|---|
| Dry | Dry |
| Fair/Medium | Wet (Dry Snow $<$ 20 mm) |
| Good | Packed Snow Compacted Snow |
| Poor | Wet Snow, Slush, Standing Water, Ice |
| Nil | Wet Ice |

### 1.3.2 Runway Contaminant Type and Depth Observations

Runway Contaminant Type and Depth Observations are typically conducted by the airport operations personnel. This is commonly used for determining the condition of the runway surface. Observers experience and vantage point are subjective and the rapidly changing weather conditions from the time of observation introduce variability in the observation results. FAA has yet to determine the correlation between aircrafts ability to brake with the Runway Contaminant Type and Depth. More often the results of this report can be useful when Ob-Board Performance Computer (OPC) needs specifics, such as the type and depth, of the contaminant as an input to provide landing distance assessment to the pilot during the time of final approach to the runway. It is very important to determine the

[3]Under extremely cold temperatures, these relationships may be less reliable and braking capabilities may be better than represented. This table does not include any information pertaining to a runway that has been chemically treated or where a runway friction enhancing substance has been applied.

difference between dry or wet snow and slush conditions due to the difference in affect they have on the braking ability of the aircraft. Airport operators are not required to report snow, ice, standing water or slush under 0.01 mm when a very thin layer of ice can surely change the stopping behaviour of the aircraft. European Aviation Safety Agency (EASA) recommends analytical way to model the effect of the contaminant on the landing distance by observing the type and depth of the contaminants. EASA considers standing water, slush, wet snow, dry snow, compacted snow and ice as contaminants on the runway. By observing the condition, different approaches are taken to estimate the effect of various contaminants on aircrafts stopping performance [10].

### 1.3.3 Ground Surface Friction Measurement Devices

Ground Surface Friction Measurement Devices were mainly developed to be used for maintenance purposes on the runway, not for estimating aircraft landing performance. These devices are useful to determine the trend in the runway condition. For instance, they can be used to determine the friction available on the runway after it has been chemically treated or cleared after precipitation. There are two types of ground surface friction measurement devices commonly used in practice for observing the condition of the runway surface during winter: Continuous Friction Measuring Equipment (CFME) and Decelerometers (DEC).

#### Friction Measuring Device Specifications

In order to establish and maintain the performance, reliability and consistency of the ground surface friction measurement devices, list of criteria, listed below, they should suffice are provided and regulated by the aviation agencies. Testing vehicle has to be portable, rugged, reliable and qualified for size, braking and suspension system, shock absorbing capabilities and tire performance. Vehicle can be front-wheel, rear-wheel or four-wheel drive, but it must not be equipped with ABS since it lowers the value of friction by distorting the sensitivity of the decelerometer. Additionally, ABS systems from various manufacturers can add the variation in the friction reading. In order to minimize the rocking and pitching motion during brake application, the vehicle should have heavy-duty

suspension system. It must meet the technical specification of measuring deceleration of the vehicle to an accuracy of 0.02g from speeds greater than 24 km/h consistently under change in vehicle velocity or contaminated runway pavement surface. Devices used in Canada include the Mechanical Tapley Meter, Mechanical Bowmonk, Electronic Recording Decelerometer (ERD), Electronic Tapley Meter and Electronic Bowmonk.

Continuous Friction Measuring Equipment (CFME) is usually equipped with a test wheel, braking actuators and force sensors [11]. Continuous Friction Measuring Equipment (CFME) devices are useful for measuring the pavement covered with contaminants to provide a continuous graphical record of friction characteristic for the length of the runway. Mostly, the friction values are averaged for each one-third zone of the runway length. These devices can be self-contained (built into commercial vehicle) or towed and calculate tire-pavement friction coefficient by skid resistance of the instrumented test wheel which can be independently braked to induce a desired slip ratio. For busier airports, decelerometers are the recommended type of ground surface friction measurement devices since they do not require the full length of the runway. It is also beneficial in the cases where the runway is crossed by another runway obstructing the airport operations from accessing the full length of the runway. They do not provide a graphic record of the friction unlike Continuous Friction Measuring Equipment (CFME). Decelerometers should only be operated on contaminated area of the runway pavement in order to provide conservative runway braking conditions.

### Friction Measuring Procedure

Before carrying out the runway surface friction test the operator has to ensure that the device has been calibrated and ATC has been coordinated for such activity on the runway. Runways serving bigger aircrafts and smaller aircrafts should perform the friction test 6m and 3m from the runway centerline, respectively in the same direction as the planes are landing. Unless, both sides of the centerline are noticeably different the test can be performed on either side. The tests are to be conducted on three zones of the runway, named according to the landing direction: Touchdown, Midpoint and rollout zone. There are minimum of three readings required in all three zones of the runway which are averaged

to provide one reading per zone. After these readings are available to the airport operations the Canadian Runway Friction Index (CRFI) or International Runway Friction Index (IRFI) are used to correlate ground surface vehicle measurement to aircraft performance for certain contamination conditions. Over the years friction testers have found their way into runway surface condition reporting process. Many airline operators have developed tables to correlate friction measurement to Braking Action Reports (BAR); however Boeing does not support this approach. Federal Aviation Regulations (FAR) strictly forbids airport operators from attempting to correlate the value read ( Number) by the devices to Good/Medium (Fair)/Poor or Nil or any type of Braking Action Reports (BAR). It was suggested in safety recommendation after the incident at Chicago Midway International Airport that ground friction measurement devices should not be used to measure aircraft stopping performance. There is variability in the calibration and design of these equipments since they are manufactured by various manufacturers. Changes in temperature, sunlight, precipitation, accumulation and operating traffic add to the variation of the pavement condition. The friction measurement taken 30 minutes prior to the overrun incident at MDW airport was less conservative compared to the braking action report. It reported a  value of 0.67 which correlated to bare and dry runway condition according to the Canadian Runway Friction Index. A reading taken right after the accident showed a  value of 0.40 which is considered fairly good. Friction measurement readings for the surface with 3 mm of lose snow ranged from 0.16 to 0.76 with the use of the friction tester. The wide range of measurements with a single type of contaminant demonstrated that this equipment is not reliable to predict aircraft braking ability under bad weather conditions.

## 1.4 Observations and Limitations

Airline operators should be able to relate the braking ability of the aircraft with any of the three runway surface condition reports to validate aircrafts landing performance. Since the airline operators use third-party data and methods developed by them variable estimates of aircraft landing performance and different safety margin are used even for the operators of aircrafts of identical model and make. Many times, due to the flexibility allowed to airline operators in selecting choice of method for interpreting the surface condition reports one

flight crew using similar aircrafts and similar runway is permitted to land while another is not. All methods currently used have limitations, regardless of the method used, due to precipitation, accumulation, traffic, direct sunlight, temperature variations, or runway maintenance/treatment runway surface conditions may vary over time. The aviation agencies do not have a method to correlate aircrafts braking ability to runway surface condition that is universally accepted to this date [12].

Many of these factors are uncontrollable and unavoidable, but mitigating the risk of runway excursion due to runway operations inability to effectively report the condition of the runway is achievable. Here, best possible way to find the friction coefficient felt by the aircraft would be to collect data from the identical aircraft under the same conditions [3]. It was suggested that aircraft-based friction measurements should be used to quantify the condition of the runway pavement under bad weather conditions. It was evident that data from FDR after overrun incidents was very useful in determining the condition of the runway surface and braking effectiveness. This way data from an aircraft that landed successfully can be used to perform rational arrival landing distance assessment for the trailing aircraft once the type, loading, configuration, braked wheel configuration, and antiskid efficiency differences have been correlated. These practices are worthy of quantifying aircrafts braking ability and runway surface condition if particular parameters of interest are recorded and studied, even at low speeds.

This thesis discusses the device, Braking Availability Tester (BAT) along with its components. BAT architecture is discussed in detail to provide an overview of the functionality of the system. Experimental data is further analyzed to show the validity and operation of the device. Also, it discusses a new method to help quantify the braking availability on the runway in order to help the pilot make more insightful decision about landing the aircraft under poor weather conditions.

# Chapter 2

# Architecture of the BAT

The BAT is built on top of a test vehicle, Ford F-350 truck, which will be driven on the runway for monitoring the road condition. Figure 2.1 shows the overview of the BAT. The test vehicle is shown in Figure 2.1(a). The main part of the BAT is the instrumented wheel that is installed near the drive shaft under the bed of the truck as shown in Figure 2.1(b). This wheel assembly is equipped with a suite of sensors (encoder, load cells, pressure transducers and linear transducer) to collect various information that contributes to the braking availability. The vertical movement (touch-down and take-off) of the instrumented wheel is realized by the embedded controller located between the passenger seat and the driver seat (the wired box in Figure 2.1(c)). The embedded controller also processes all the sensory information and is under the control of the host PC (the laptop) which will be operated by the airport personnel.

## 2.1 Hardware Configuration

The instrumented wheel in Figure 2.1(b) is assembled to the underbody frame of the F-350 truck. Total weight of the truck is around 5,700 kg (curb weight of the truck: 3,000 kg; steel ballasts: 1,100 kg; BAT assembly weight: 1,600 kg). The weight provides the stability during the application of vertical load and braking action to the wheel. The instrumented


(a) The BAT is built on F-350 truck.

(b) Instrumented wheel touching the ground.

(c) Control system located in passenger seat.

Figure 2.1: Overview of the BAT

wheel can be lifted up or lowered down using the hydraulic cylinder and the parallel linkage mechanism pivoting about the structures fixed to the truck frame. Figure 2.2 illustrates the vertical movement of the wheel. After the wheel is touched to the ground, the hydraulic cylinder can further apply the vertical load by increasing the hydraulic pressure. The BAT is designed to provide up to 2,500 kg of vertical weight which will be around 10% scale-down from that of the Boeing 737-100. To mimic the aircraft braking system, the actual aircraft tire has also been used. Due to the space limitation under the truck frame, a nose

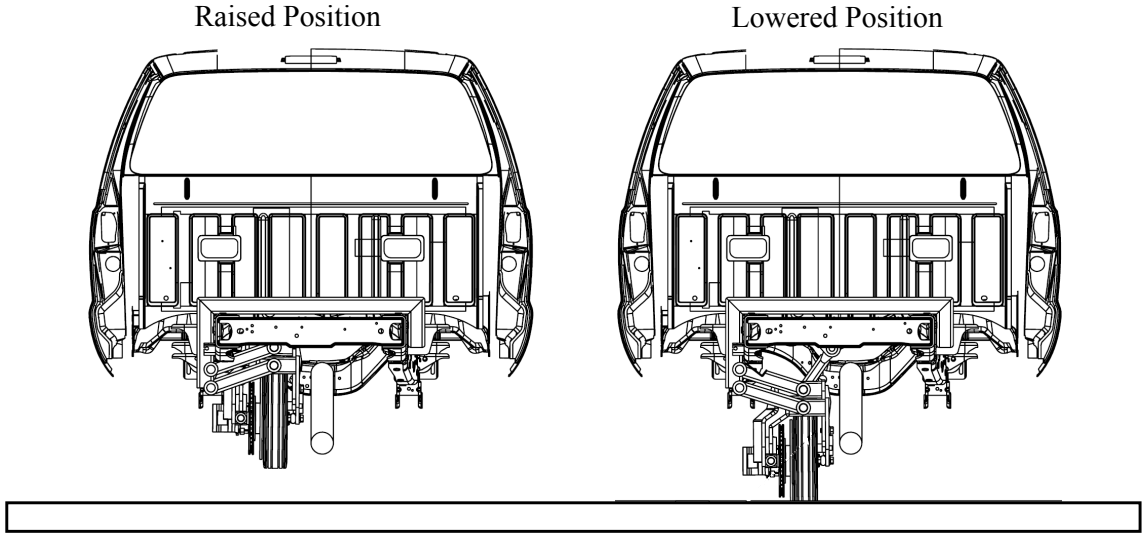


Figure 2.2: Vertical movement of the instrumented wheel.

gear tire has been adopted instead of the landing gear one. More detailed view of the wheel assembly is shown in Figure 2.3 where the brake assembly and some of main sensors are also indicated. The left-hand side of Figure 2.3(b) shows the brake assembly. The status of the brake is monitored by the brake pressure sensor, the wheel speed sensor and the temperature sensor. The wheel speed sensor is particularly important as a feedback signal for the antiskid braking system (ABS) controller. The primary feature of the brake system in the BAT is that it is equipped with the actual aircraft brake control valve (BCV) that is currently used in passenger aircrafts. It is a current-controlled servo valve manufactured by Crane Aerospace & Electronics and is capable of high speed operation of the brake calipers, which is essential for high performance ABS operation.

The BAT is instrumented with a number of different sensors. The most important information is provided by the three load cells: horizontal, vertical and torque as shown in the right-hand side of Figure 2.3(b). Horizontal load cell measures the drag force resulting from the tire-pavement interaction when a brake force is applied while the torque load cell directly measures the braking torque. The drag force reflected to the horizontal load cell will depend on the brake torque as well as the vertical load, the variation of which is monitored by the vertical load cell. Other important measurements from the BAT include

the hydraulic pressure at various locations (the vertical load cylinder, the brake servo valve, and the return port), the brake rotor temperature (to compute the brake energy), runway temperature, the vehicle speed (Global Positionaling System: GPS), accelerometers, and the potentiometer (to measure the stroke of the vertical cylinder).

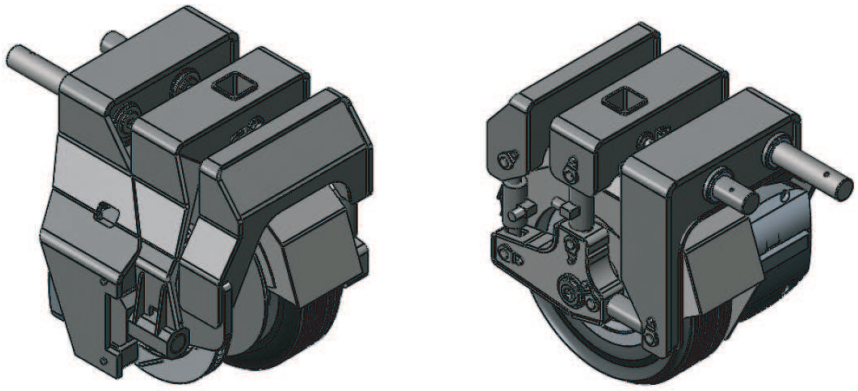

(a) Isometric view of the wheel assembly

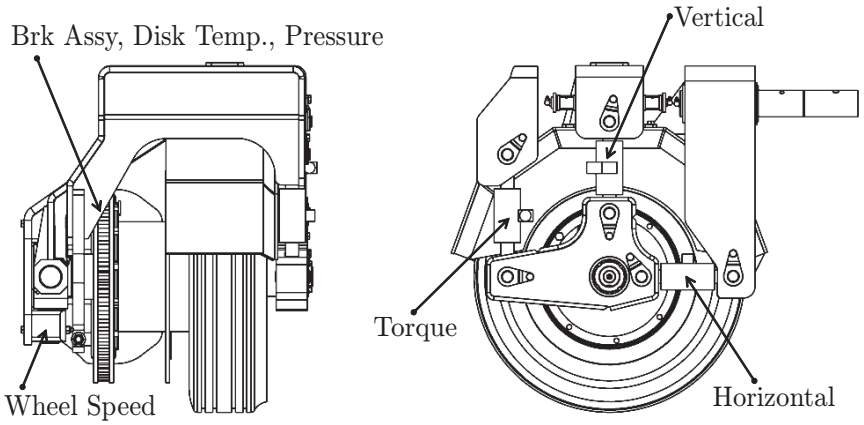


(b) The brake hardware and main sensors

Figure 2.3: BAT wheel assembly.

## 2.2 Operational Principles

The BAT is operated by two functional subsystems: the data acquisition (DAQ) system and the BCS. The DAQ can further be broken down to two main components: LabView and *PLUS+1*. LabView is at the top most level which has control over all the other components. PLUS+1 is a great solution that provides easy interaction with heavy duty hydraulics. On the other hand, the BCS produces and regulates the control signal for the BCV in order to avoid wheel slip while operating at maximum drag producing conditions. All the operational functions of the BAT are implemented using the Compact Realtime Input-Output (cRIO) system and LabView programming language provided by National Instruments Inc. The cRIO is mounted to the inside of the main control unit shown in Figure 2.1(c). It operates through a deterministic realtime (RT) control loop running at 3 millisecond of sample time. The operation of the RT control loop can be monitored or commanded by the operator through the host laptop computer shown in Figure 2.1(c). After data collection, LabView executes the BCS on the Field-Programmable Gate Array (FPGA) of the cRIO to produce necessary output to the actuators. The sequence of events in the 3 millisecond can be described as shown in Figure 2.4. There are other components such as PLUS+1 and BCV current driver involved in the instrumentation that run in parallel to make the system work. LabView, cRIO and PLUS+1 are the most important parts of instrumentation. LabView and cRIO are integrated to work together, while PLUS+1 is an external part. PLUS+1 is mainly used to read/write signals received from/to LabView. LabView is at the top most level on the control topology. All the control and input signals generated by the BCS are sent by LabView and all the system outputs

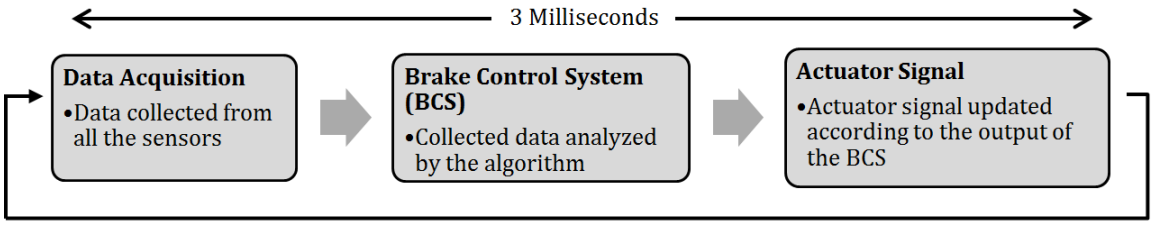


Figure 2.4: Sequence of events within one cycle.

are monitored in real-time. cRIO's ability to operate at high sampling period has made it possible to implement the BCS. PLUS+1 does not have the ability to change input signals at high frequency which is crucial for implementation of BCS. Moreover, cRIO that is used with the system can have up to six modules attached to it, once the chassis is provided. Out of these six modules one can pick and choose which modules (Analog I/O or Digital I/O) are useful for the application. Three main modules used with the cRIO are listed in Table 2.1. All these modules have high resolution to provide accurate sensor reading and actuator output command. PLUS+1 improves accessibility to most of the sensors and actuators used

Table 2.1: Modules used with cRIO *(National Instrument Inc. 2013)*

| **Module** | **I/O Used** | **Purpose** |
|---|---|---|
| NI 9205 Analog IN | 12 Single Ended Analog Inputs | Pressure Transducers, Load Cells, Accelerometer, Linear Potentiometer, Temperature Sensor |
| NI 9401 Digital I/O | 3 Digital IN, 8 Digital OUT | Solenoid ON/OFF Valves, Wheel Speed Sensor, GPS Speed Sensor |
| NI 9263 Analog OUT | 2 Analog OUT | Proportional Valve Control, Brake Control Valve (BCV) |

in the BAT by providing compliance packages. These compliance packages allow one to seamlessly integrate electrical and hydraulic components while having customized control system. In this case, all of the control is provided by LabView and cRIO which passes the signal to either digital or analog pins of PLUS+1 microcontroller. After interpreting the input signal, PLUS+1 using the compliance package generates digital or analog output to the appropriate actuator. PLUS+1 is very useful in operating ON/OFF solenoid valves, due to its current amplification ability. For instance, to increase the vertical load to the BAT wheel, analog signal from cRIO is sent to PLUS+1. PLUS+1 microcontroller reads this signal and amplifies the current to the vertical actuator to provide a greater load at the BAT wheel. More importantly, all the detailed specifications and other related information regarding the actuator is not required by LabView since this is taken care of in PLUS+1. PLUS+1 compliance blocks maximize productivity and LabView comfort by providing a responsive and simple interface. Thus, after receiving the feedback information from the

sensors, the BCS can send out appropriate actuator signal at 3 msec rate (made possible due to cRIO). This in turn will produce the output required at the actuators helping the system function.

## 2.3 BAT Hydraulics

BAT is controlled hydraulically with the use of two pumps and with the hydraulic fluid returning to the same reservoir. There are two main parts to the hydraulics system: Braking Side and Landing Side. Braking side is essential for smooth operation of the BCS. The landing side controls the vertical position of the BAT wheel (lifted or lowered) and the load on the BAT wheel. Both parts of the hydraulic circuit are shown in Figure 2.5. System pressure of 3000 psig is maintained and monitored by pressure transducer (21E). Accumulator (15) and the two-stage filters (F3 and F4) at the beginning reduce the variations in the pressurized flow.

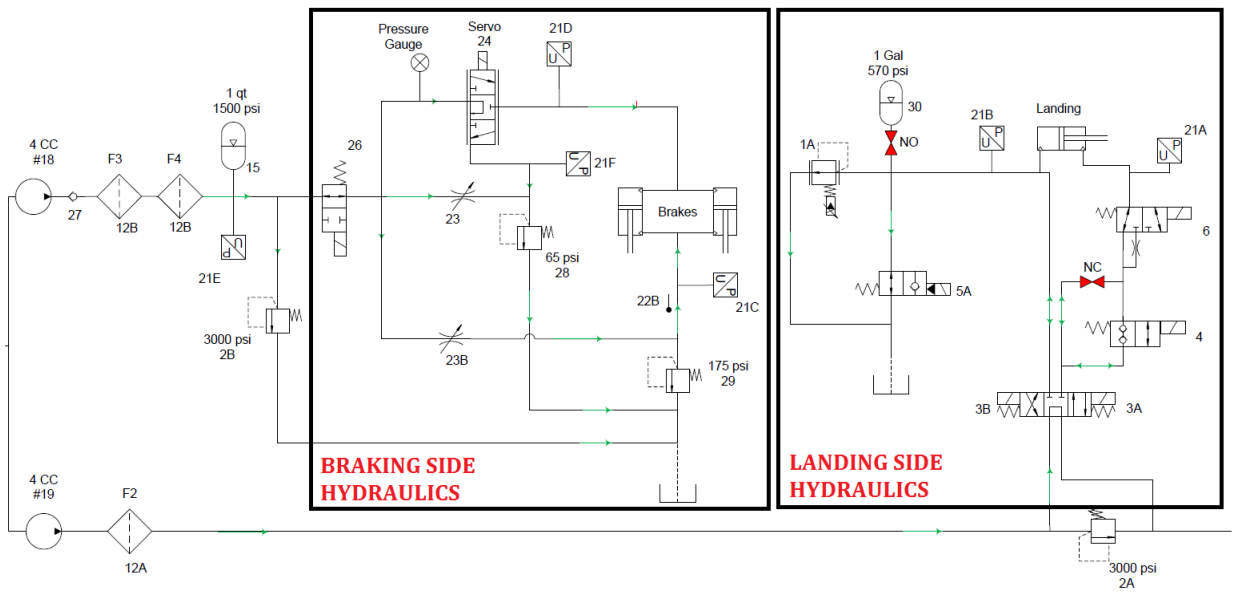


Figure 2.5: BAT Hydraulic Circuit. *(Team Eagle Ltd. 2013)*

### 2.3.1 Braking Side Hydraulics

Braking side of hydraulic circuit ensures that pressure applied to the brake cylinder at the brake calipers generates the brake force required by the BCS. It is essential that the flow to the BCV is continuous and variation free. Once the BCV has a steady flow to it, controlling the brake pressure, monitored at 21D, generated by the BCV becomes easier. This is made possible by maintaining a return pressure between 60 and 80 psig read by the pressure transducer 21F. The back pressure measured at 21C, is the pressure that the BCV has to overcome in order to make contact with the brake rotor disc and start applying brake force. This is to provide the brake algorithm extra space to deal with situations when slip is occurring. Most of the time when there is no signal from the BCS the brake calipers are retracted back from the rotor disc to allow free motion. To facilitate this type of behavior the brake caliper housing has been modified to have two-way pistons, this allows one to retract and extend the brake pads to apply or release brake force when required. More importantly, back pressure can be used to deal with the cases where the BAT wheel locks up and extra space is needed for the wheel to fully start rotating again. There is a safety valve (26) installed just before the BCV to make sure that the BCV does not get damaged in case of unstable flow, sudden changes in pressure or failure of a component in the hydraulic circuit. This valve is normally open, but as soon as it is actuated all the flow to the BCV is stopped. Thus, the braking side hydraulic circuit dictates how the BCS performs.

### 2.3.2 Landing Side Hydraulics

Landing side hydraulic circuit is designed similarly in a way that 1 gallon accumulator (30) is installed to provide vibration less and continuous flow to the vertical load cylinder. When the BAT truck is moving there are variations introduced due to the profile of the road. The accumulator acts as a damper to dampen out this effect as much as possible. Two-way valve (3A and 3B) controls the position of the BAT wheel. Vertical load cylinder (Landing) decides the amount of force that is applied on the BAT wheel. 21B measures the corresponding pressure required to produce the required load at the BAT wheel. Slow lowering valve (6) helps ensure that there is no damage caused to the BAT wheel when

it is being lowered to the ground. If energized, the flow will pass through the metering valve, resulting in a smoother and slower vertical displacement of the BAT wheel. Valve 4 is used to lock the BAT wheel in its current position. Hydraulic fluid cannot flow through, so that the landing gear can be held at the current position for a long time. Being able to control the vertical load is crucial for the application of the BAT since different aircrafts vary in terms of the weight that they land with. Since the brake force that can be applied is limited, controlling the vertical force becomes crucial. Moreover, the braking pressure is regulated by maximum system pressure which makes the vertical load the main variable to modify. There are many other limiting factors that can limit the functionality of the BCS, but having the ability to change the vertical load can help the system adjust under various weather conditions.

## 2.4 BAT Wheel Speed Transducer

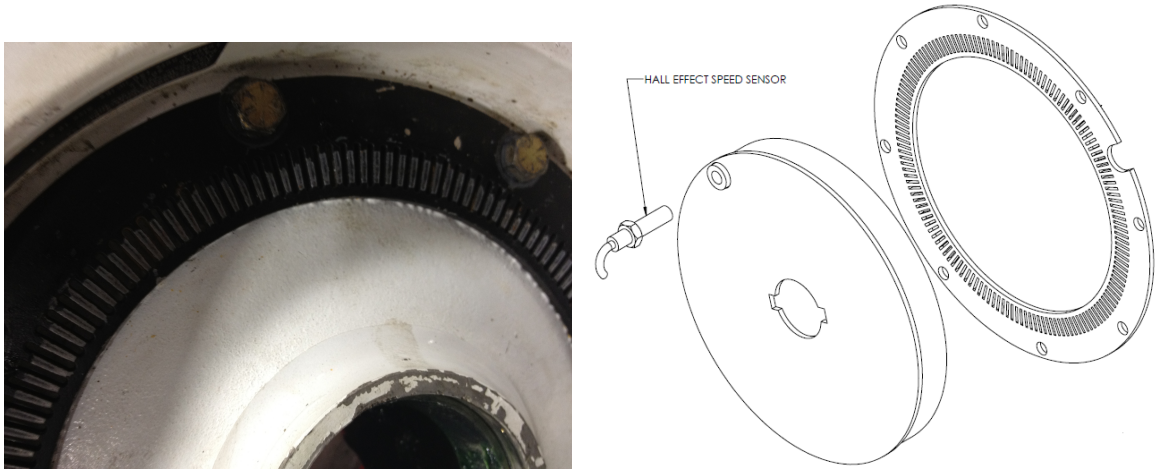


(a) Exciter disc with grooves.

(b) Hall effect sensor assembly.

Figure 2.6: Hall effect speed sensor. *(Honeywell Inc. 2013)*

BAT uses a rotary encoder sensor to measure the speed of the BAT wheel. The exciter disc is made out of iron in order for the Hall Effect sensor to work. The setup is as shown

in Figure 2.6. Figure 2.6(a) shows the actual BAT wheel with the exciter disc mounted to it, where Figure 2.6(b) shows the assembly of the sensor.

It is essential to have a clean BAT wheel speed signal in order for the BCS to operate successfully. The resolution of the exciter disc and the speed of the BAT wheel play a major role in determining the quality of the signal. The BCS will not be able to operate successfully due to the continuous and unexpected changes in the speed reading of the BAT wheel. Moreover, the resolution of the exciter disk is 150 Ticks/Rev, which is low for high precision measurement of the speed, especially at lower speeds.

There are two methods that can be implemented to measure the speed of the wheel. Method 1 takes into account the period of the square wave and converts this time period into linear speed. This method yields good results at low speeds, but as the speed of the BAT wheel increases the period of the signal generated by the encoder gets smaller, while introducing noise since any small change in period could cause the speed reading to change. For instance at the linear speed of 91 km/h the period of the square wave generated was 0.31568 msec. However, this means that any small change in the period could cause change in the speed reading of the wheel. Thus, method one introduces noise at high speeds. Method 2 has a constant sampling period in which the rising and falling edges of the encoder signal are summed. Once the number of ticks in a constant period is available, speed of the wheel can be calculated. It is evident that at lower speeds this method is not robust because the numbers of ticks detected in a constant period for various speeds could be the same. For example, speed of 11.49 km/h generates a square wave with a period of 3 msec with 50% pulse width. If one is measuring the number of ticks at a fixed period of 3 msec, then total number of ticks detected would be 1, which converts to 11.49 km/h. However, at speeds lower than 11.49 km/h only 1 tick would be detected resulting in the same speed reading. On the other hand, at higher speeds the number of tick counted per 3 mSec vary greatly due to the high frequency square wave generated by the encoder. For example, at 91 km/h the period of the square wave is 0. 7576 msec and ticks detected are 7.9. At 92 km/h the period of the square wave is 0.7494 msec and the tick count is 8.

Currently, the speed is being measured by looking at the period of the square wave signal (method 1) coming from the encoder; this period is converted to linear speeds in

real-time. From Figure 2.7 it is visible that the raw wheel speed signal is noisy. Due to limitations at the moment, a software solution that includes a 21Hz low-pass filter for disturbance elimination and a notch filter is used in order to deal with the resonance of the system. The raw speed signal goes under a low pass filter and a notch filter before being processed by the BCS to improve the quality of the signal without losing information. The filtered signal eventually used by the BCS is shown in Figure 2.7(a). It can be seen that the filtered signal has lower noise on it compared to the original raw signal. It is more evident in the magnified view shown in Figure 2.7(b). In order to further improve the quality of the speed signal the encoder exciter disc could be replaced with a higher resolution encoder disc to give out more ticks in 3 msec. This would help improve the quality of the speed signal at lower speeds. Moreover, the BCS could be programmed to use method 2 at low speeds and method 1 at high speeds.

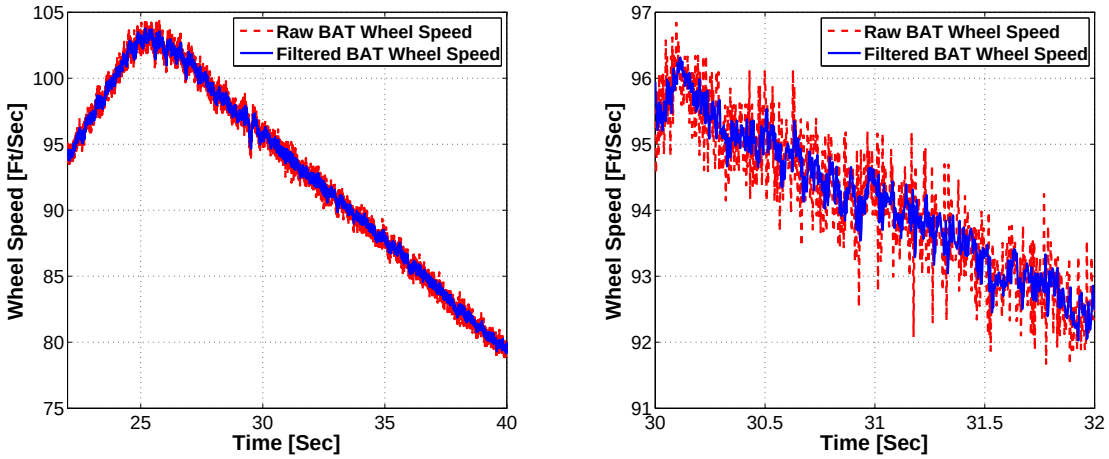


(a) Wheel speed signal.

(b) Wheel speed-Magnified.

Figure 2.7: Wheel speed filtering

## 2.5 Pressure Transducer

The pressure transducer shown in Figure 2.8(b) is used to monitor the pressure at various locations in the hydraulic circuit. All of these pressure transducers are designed for heavy duty application which increases the reliability of sensing. More importantly, the pressure transducer has compliance block that can be used with PLUS+1 to take advantage of its functions and calibration process. Moreover, the pressure to voltage relationship is linear as shown in Figure 2.8(a) which makes the calibration easy for application in LabView. The range of the pressure transducer is 0 to 3262 PSI [0 bar to 250 bar] which is the right fit for application since the pressure of the system does not go over 3000 PSI. In Figure 2.8(c) modulation in the brake pressure signal is visible. Since the low-pass filter implemented on the pressure feedback signal has a cut-off frequency of 50 Hz, this signal is unaffected. This is why there is no difference between the filtered and unfiltered brake pressure signals. It is important that the smallest possible variation is read by the sensor because the brake pressure is the most important control signal used in order to observe the condition of the runway and generate required drag.

## 2.6 Linear Potentiometer

Linear potentiometer is an important part of the BAT assembly because it measures the lateral position of the BAT wheel using the BAT vehicle frame as the reference. Moreover, bumps and vibrations to the BAT wheel can be seen from the signal provided by the linear potentiometer. This can help understand the variations in the vertical load and drag force caused by the condition of the runway. The potentiometer used in the BAT assembly is as shown in Figure 2.9. The signal from the liner potentiometer for a full test run is shown in Figure 2.10. From the data it can be seen that there is vibration in the system. Moreover, this signal can be used to verify if the BAT wheel has lowered safely onto the ground and the vertical load has been applied to it(See Figure 2.10(a)). From the current test it can be seen that, after 20 seconds, there are no vibrations introduced to the BAT wheel while it is running. However, upon closer examination one can see that during braking application the position of the BAT wheel changes (See Figure 2.10(b)).

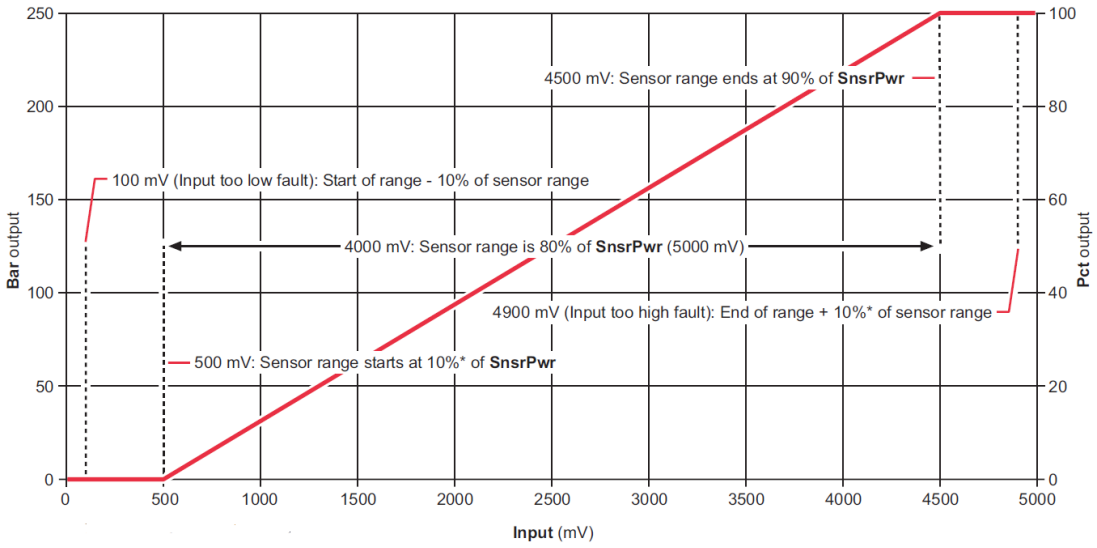


(a) Pressure vs. voltage relationship.

(b) MBS 1250 heavy duty pressure transducer.

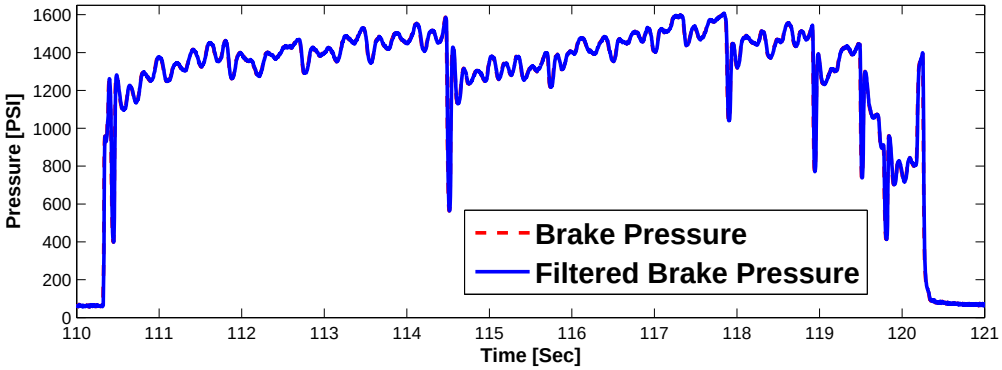


(c) Brake pressure signal.

Figure 2.8: Overview of the pressure monitoring transducers. *(Sauer-Danfoss 2009)*

Figure 2.9: Linear potentiometer.*(A-Tech Instruments Ltd. 2008)*

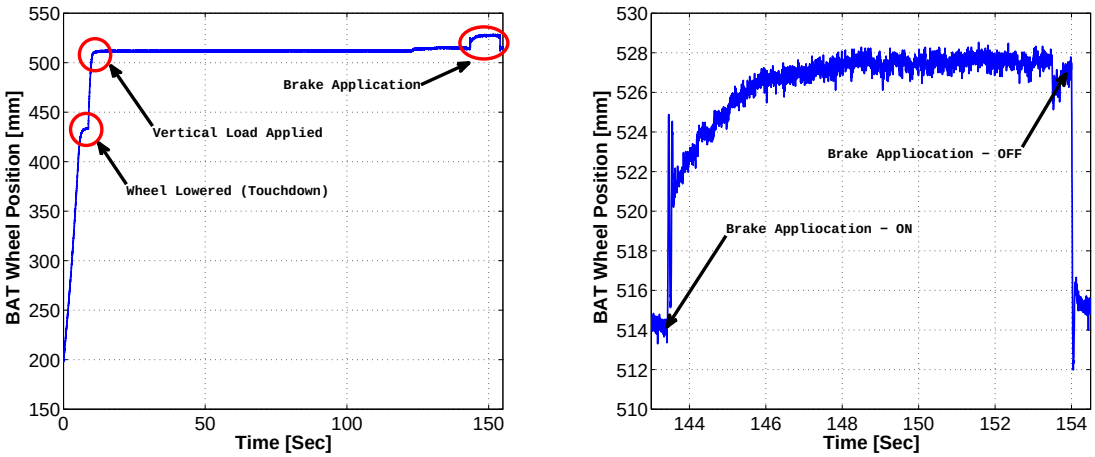


(a) Linear potentiometer signal (Full Test). (b) Linear potentiometer signal (During Braking).

Figure 2.10: Linear transducer signal.

## 2.7 Load Cells

Load cells are the most important part of the BAT wheel assembly (See Figure 2.11) due to the information they provide. Horizontal load cell provides the drag read on the runway, vertical load cell measures the load applied to the BAT wheel, while the Brake torque load cell can be used to monitor the torque generated by braking the BAT wheel. Brake torque load cell can also be used to revaluate the drag read by the horizontal load cell. Load cells used in the BAT assembly are model RGF provided by Honeywell shown in Figure 2.11(a).

These load cells are strong enough to hold off-axis loading. This is important for the BAT wheel since in-line tension and compression measurements are made, but the side loading can not be completely controlled. Moreover, there are various types of connections that can be used to connect the load cells with the structure: Tongue shackle male, Rod

end bearing male, Yoke shackle male. Additionally, the material the load cells are made of is stainless steel which will provide durability while testing in bad weather conditions. The models used for the BAT are within the 2000 to 5000 lbs range. Figure 2.11(b) shows how individual load cells are setup in the BAT system. In-line amplifier provided by Honeywell is used to amplify the signals coming out the load cells. The amplifier is operating in 0 to 5 Vdc range for each specific load cell. It is important to let the amplifier warm up before the first test run in order to get valid data. 0.25% accuracy of the output was one of the main reasons these load cells were used[13]. This will ensure that the drag and brake torque readings are accurate.

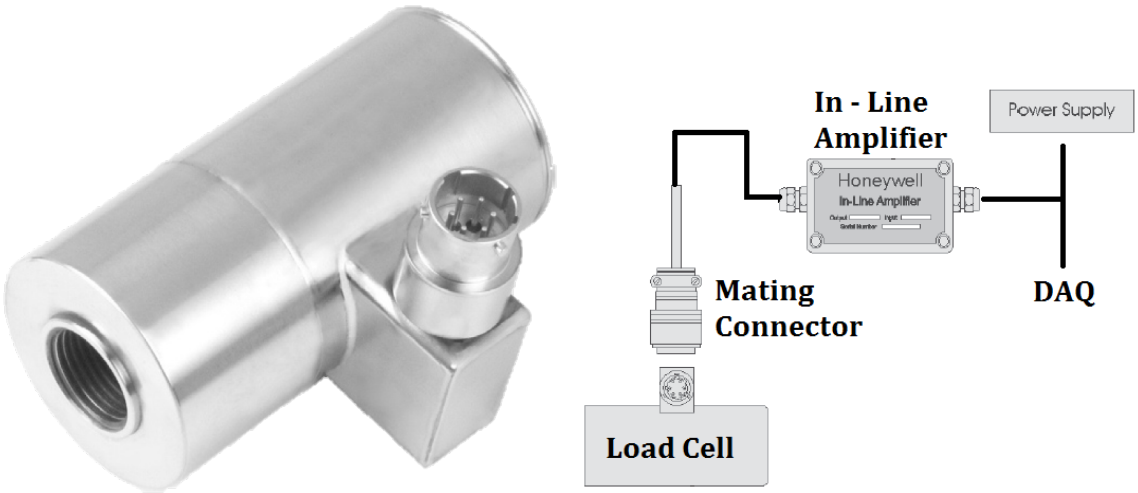


(a) RGF Load Cell.

(b) Load Cell System Diagram for the BAT.

Figure 2.11: Load cells in the system.*(Sensing and Control Honeywell Inc. 2010)*

# Chapter 3

# Operation of Aircraft- Like Braking System

This chapter discusses the components that make the BAT different. It discusses the BCV extracted from an actual aircraft braking system. System identification of the BCV in the BAT hydraulic circuit is explained in detail. Techniques used to generate non-parametric models that fit the behaviour of the BCV are shown. The results from each model are compared to the experimental data for validation. The best model fit is selected from all the non-parametric model developed. The control strategy implemented to control the barking of the BAT wheel is explained. The architecture of the BCS developed by Meggit Aircraft Braking Systems Corporation is discussed.

## 3.1 Brake Control Valve (BCV)

The Brake Control Valve (BCV) is the main and the most delicate component of the BAT architecture. Due to Brake Control Systems (BCS) dependability on the BCV for controlling the braking applied to the BAT wheel, it is also the most essential part of the BAT hydraulic circuit. The BCV, manufactured by Crane Aerospace and Electronics, is a Line Replaceable Unit (LRU) from the BCS of Bombardier BD -700 Global Express

aircraft. The particular model of the BCV used in the BAT is 39-815; the make-up of this model is shown in Figure 3.1(a). The hydraulic and electrical schematic of the BCV can be seen in Figure 3.1(b). The BCV meters aircraft hydraulic system pressure to control power braking in response to movement of the brake pedals. When commanded, the BCV also modulates the applied brake pressure to provide antiskid protection. The first-stage of the BCV is an electromechanical device, which includes a single coil that controls pressure and return nozzles as a function of command current from the Brake Control System (BCS). The electrical circuit is made by connecting the port A and B of the electrical schematic shown in Figure 3.1(b) to the current amplifier that receives commands from the Brake Control System (BCS). The hydraulic ports are machined into the single cast aluminum body and identified with PRESS (System Pressure), BRAKE (Brake Port Pressure), and RETURN (System Return). The PRESS port connects system pressure of 3000 psig while the RETURN port connects to system return pressure. The BRAKE port connects to the brake line that is connected to the brake caliper assembly of the BAT wheel. The BCV is a current-controlled device that operates in a range from 0 to 55 mA, for BAT purposes braking pressure produced by 40 mA of current is used. The envelope that the Brake Control Valve (BCV) operates in is shown in Figure 3.1(c); it needs to be tuned by adjusting the screws accessible by removal of the cover to set the applied brake pressure versus control current curve. It is important that the BCV operates within the upper limit and the lower limit. Otherwise the valve needs to replaced, this can easily be done since the BCV is a line Replaceable unit.

The pressure at the BRAKE port increases when the Brake Control System (BCS) increases current to the Brake Control Valve (BCV). The BCV changes brake pressure in proportion to the strength of the control command. The pressure port supplies hydraulic fluid under pressure through the servovalve assembly to the slide. When the torque motor flapper is in the neutral position, system pressure is greater at one end of the slide. This built-in bias holds the slide in a position that allows flow from the PRESS port to the BRAKE port. The second stage slide and sleeve lap assembly shown in Figure 3.1(b), is a high-tolerance lap fit assembly. The highly polished surfaces allow the slide to reposition in the sleeve in response to pressure changes without internal leakage. In order to confirm the specifications and operation of the BCV, several tests need to be done. Moreover, it

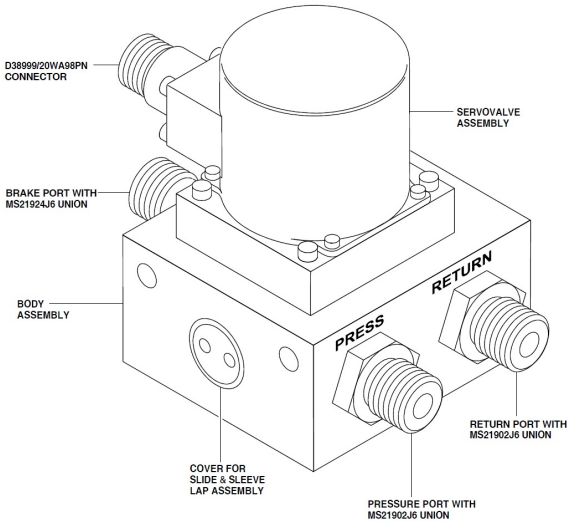


(a) Isometric view of the BCV.

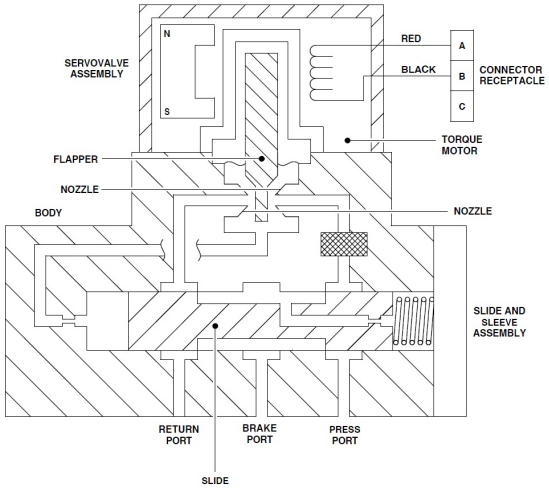


(b) Electrical and Hydraulic Schematic of BCV.

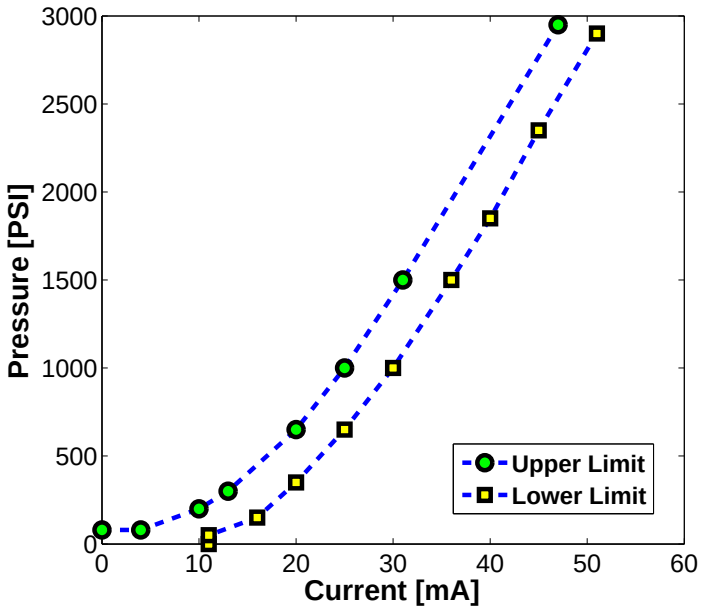


(c) Operational envelope of the BCV.

Figure 3.1: Brake Control Valve (BCV) *(Hydro-Aire, Inc. 2009)*

is very important to model the Brake Control Valve (BCV) due to the impact that it has on the overall performance of the BAT. Once the BCV is modeled, further braking control strategies can be designed to use the BCV efficiently. All this development can be done offline once the model of the BCV is available. Implementation can be done at a later stage depending on the accuracy of the model. The test setup during these tests and data collection stage was as shown in Figure 3.2.

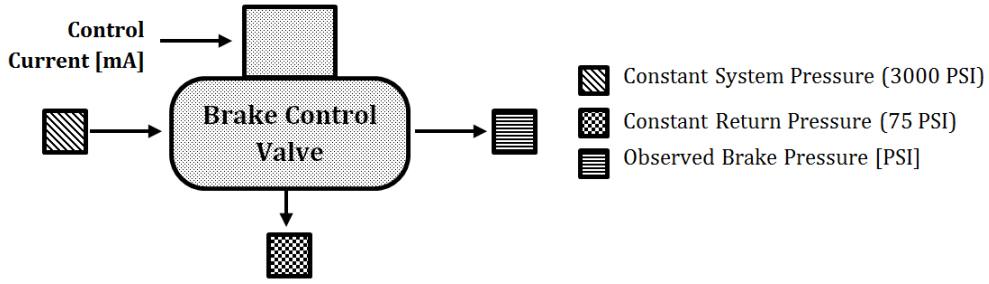


Figure 3.2: Brake control valve test setup.

## 3.2 Hysteresis of the BCV

First test was done to identify if the performance of the servo valve satisfied the operating envelope specified as shown in Figure 3.1(c). Different current commands were sent to the valve while maintaining the system pressure at 3000 psig and return pressure at 75 psig and the brake pressure was continuously monitored at the BRAKE port with the use of a pressure transducer. Analyzed data from the test is shown in Figure 3.3. It is visible that some of the pressure produced in open-loop are very close to the upper limit, but the performance of the valve is within the limits of the envelope specified. It is also clear that the gain of the valve is not linear. There is almost no hysteresis present in the valve behaviour which is really important information since this is what will dictate the accuracy of the valve when it is controlled by the Brake Control System (BCS).

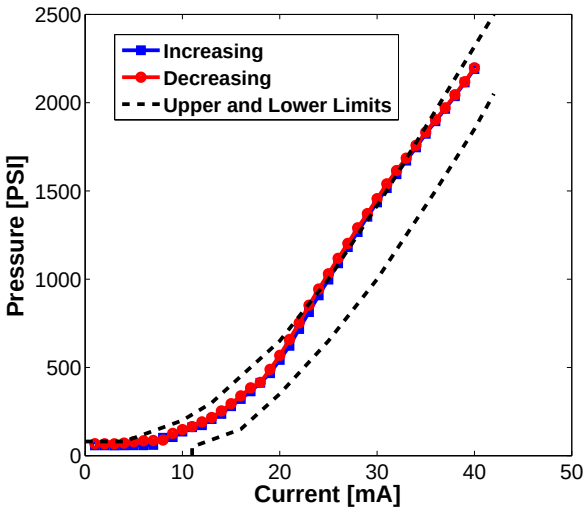


Figure 3.3: Hysteresis and envelope fit check.

## 3.3 System Identification of the BCV

In order to identify and understand the behaviour of the Brake Control Valve (BCV), it must be modeled. There are various techniques that exists that can help in one identify the system. Firstly, Least Square Estimation (LSE) was used to identify the system followed by frequency response approach. Moreover, non parametric approach was taken to match the system behavior in order to come up with the model of best-fit. The following sections discuss these approaches in detail and all the analysis that was carried out to settle to the final model of the Brake Control Valve (BCV) which was used later in the development of the Brake Control System (BCS).

### 3.3.1 Least Square Estimation (LSE)

Various different square waves with different frequencies and magnitudes (2mA Figure 3.4(a) and 5mA Figure 3.4(b)) were sent to the Brake Control Valve as the control current command. After retrieving the data Least Square Estimation (LSE) fit was performed to fit a first order model of the system. From Figure 3.4, it can be seen that the simulation

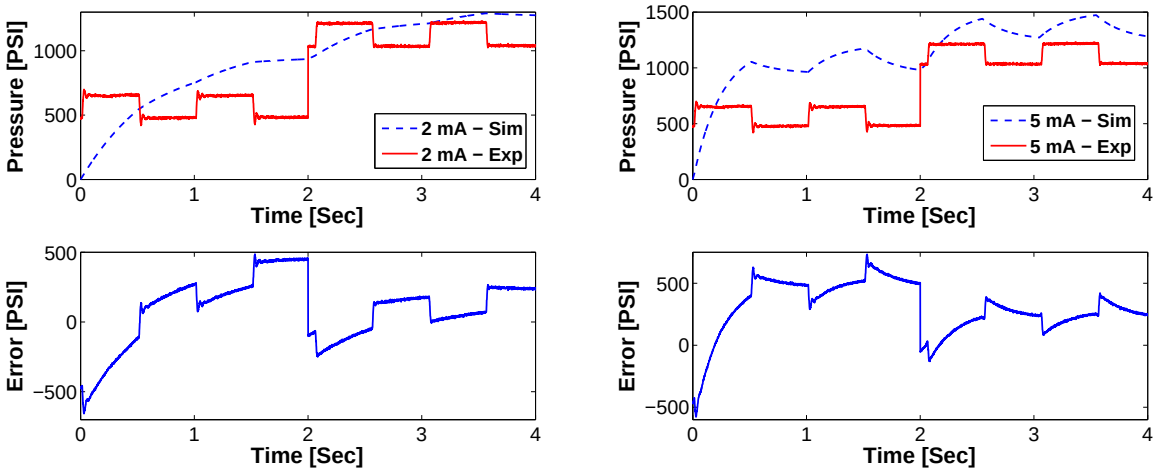


(a) 2mA control current step input.

(b) 5mA control current step input.

Figure 3.4: Least square estimation simulation results

results are not responding to the input as fast as they should and the error (Experimental versus Simulation) is very high. This confirms that the servo valve is not a firs-order system since it takes the model much longer to reach the steady state value in the simulations. Also, the experimental data shows that the steady state value for the applied current is reached much faster.

### 3.3.2 Frequency Response

Second approach taken to identify the system was through frequency response. Usually, frequency response is one of the best approaches that can be taken to identify the system mainly because it can describe the behaviour of the system under all types of inputs. Various sine waves with different frequencies were sent as the input to the Brake Control Valve (BCV) and the output was observed at the BRAKE port via a Pressure Transducer, shown in Figure 9. The control current command was in the form shown in Equation 3.1.

$$\textbf{Control Current} = \mathbf{A}\sin(2\Pi ft) + \textit{Bias Current} \tag{3.1}$$

In order to check the validity of the model after data has been collected, the frequency test was done at several different bias currents and amplitudes (A) for all the frequencies as outlined in Table 3.1. Once the data was collected the magnitude and phase of the outputs

Table 3.1: Frequencies, Bias Current and Amplitude for Frequency Testing

| **Frequency (Hz)** | 1 | 3 | 5 | 7 | 10 | 12 | 13 | 18 | 20 | 25 | 27 | 30 | 35 | 50 |
|---|---|---|---|---|---|---|---|---|---|---|---|---|---|---|
| **Bias Currents** | | | 19 mA | | | | | 25 mA | | | | 23 mA | | |
| **Amplitudes [A]** | | | 1 mA | | | | | 2 mA | | | | 5 mA | | |

were calculated for all the inputs of various frequencies. The results of the 1mA amplitude input with various bias currents can be seen in Figure 3.5. The phase and magnitude plots for the frequency responses for all the bias currents match each other very closely, which confirms that the test setup and instrumentation was satisfactory at the time of the test. Frequency response reveals very important information about systems behaviour. A constant DC gain until the cut-off frequency ($\omega_{Cut-Off}$) of almost 198 rad/sec specifies the band-width of the system which is very crucial while designing the Brake Control System (BCS). Additionally, the phase plot can help one determine the delay of the system. Moreover, it can be seen here that there is no resonance in the system which could cause the system to have uncontrollable behaviour if not paid attention to during the design stage. The effect of non-linear gain observed earlier can be seen from the magnitude plots of the different bias currents. At 19 mA, 25 mA and 35 mA DC gains of 92.87, 90.88 and 71.24 are observed, respectively. This also confirms that the system is could be of $2^{nd}$, $3^{rd}$ or $4^{th}$ order.

Nonparametric model fitting approach was taken in order to fit a model onto the frequency response of the Brake Control Valve (BCV). An attempt to fit a $2^{nd}$ order model was made and the results of the simulations and experiments were compared. To further improve the results $4^{th}$ order model fit was generated and analyzed. Finally, the benefits of the $4^{th}$ order model were compared with the $2^{nd}$ order model. Approach taken here is strictly non parametric due to the nature of the system and inability of modeling the BCV analytically.

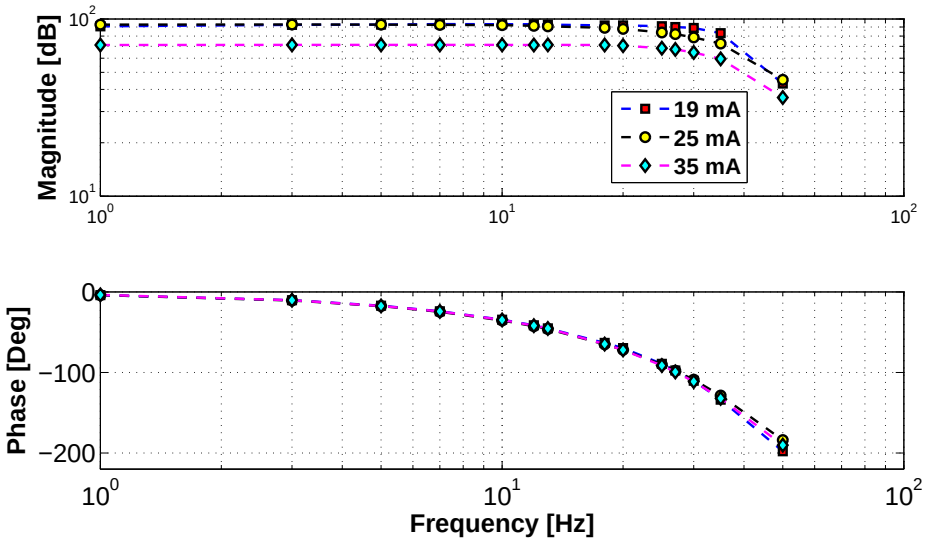


Figure 3.5: Frequency response of the BCV.

### 3.3.3 $2^{nd}$ - Order Non- Parametric Model

There were many iterations of changing the variables in Equation 3.2 in order to find the model that fits the experimental result. Finally, the $2^{nd}$ order transfer function, as shown in Equation 3.3, was used to fit onto the experimental frequency response. Here, the parameters used were $\omega_{\mathrm{n}} = 337.42$ rad/sec and $\xi = 0.707$, mainly because of no resonance in the experimental results.

$$\frac{Gain}{s^2 + 2\xi\omega_n s + {\omega_n}^2} \tag{3.2}$$

$$\frac{1.054 * 10^7}{s^2 + 477.1s + 1.139 * 10^5} \tag{3.3}$$

Figure 3.6 shows the frequency response for the experimental and the $2^{nd}$ order model fit. The magnitude plot matches the experimental results closely until the cut-off frequency. However, the phase decreases at much faster rate for the experimental results compared to the phase of the $2^{nd}$ order model.

To check the performance of this model, control current steps of 2 mA and 5 mA are sent to the model and compared to the experimental results as shown in Figure 3.7. It is

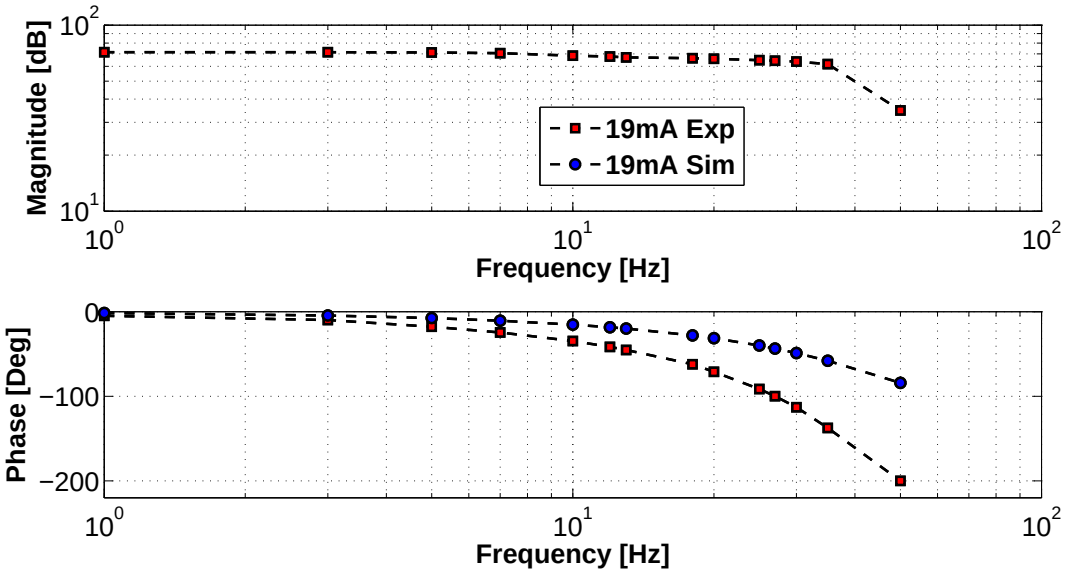


Figure 3.6: $2^{nd}$ order non- parametric Model.

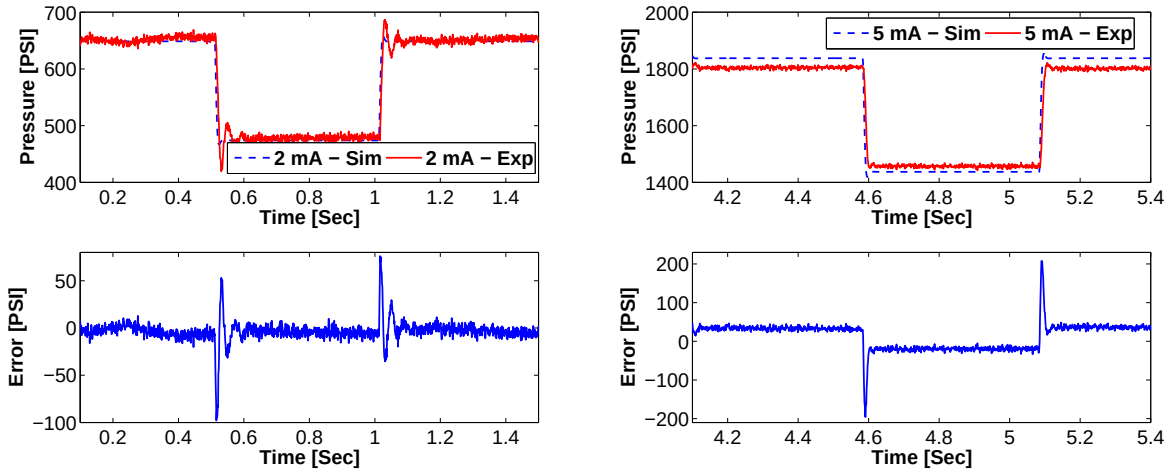


(a) 2mA control current step input.

(b) 5mA control current step input.

Figure 3.7: $2^{nd}$ order model fit simulation results

evident that the control command step changes are not applied at the same time, but from the errors one can observe that the error is much higher for the case where 5 mA step is applied. This could be the effect of the non linear gain of the servo valve. Error seems to increase as the control currents amplitude increases. For 2 mA and 5 mA steps 90 psig and 190 psig error in the brake pressure is observed, respectively.

### 3.3.4 $4^{th}$ - Order Non- Parametric Model

To further improve the model of the Brake Control Valve (BCV) in order to closely match the experimental results, a $4^{th}$ order estimate of the plant is made using a similar method used for deriving the $2^{nd}$ order model fit. For this case, four variables $\xi_1$, $\omega_{n1}$, $\xi_2$ and $\omega_{n2}$, are of importance as it can be seen from Equation 3.4. After much iteration and comparison, Equation 3.5 was the one used to fit the $4^{th}$ order model to the experimental data. Here, $\xi_1$, $\omega_{n1}$, $\xi_2$ and $\omega_{n2}$ are 0.75, 250.14 rad/sec, 0.5 and 337.42 rad/sec, respectively. The magnitude and phase plot of the $4^{th}$ order model closely matches the experimental data as shown in Figure 3.8. The phase plot is almost identical to the experimental data and the magnitude plot has the same drop-off rate after the cut-off frequency. This non parametric $4^{th}$ order guess fits the experimental data really well.

$$\frac{Gain}{(s^2 + 2\xi_1\omega_{n1}s + {\omega_{n1}}^2)(s^2 + 2\xi_2\omega_{n2}s + {\omega_{n2}}^2)} \tag{3.4}$$

$$\frac{6.593 * 10^{11}}{(s^2 + 375.2s + 6.257 * 10^4)(s^2 + 337.4s + 1.139 * 10^5)} \tag{3.5}$$

Error shows the evaluation of the performance of the $4^{th}$ order model. To look into this in more detail, 2 mA and 5 mA steps are sent as control current command on top of the same bias current. In Figure 3.9, one can observe that the error increases as the amplitude of the step is increased. For a step of 2 mA and 5 mA errors of 50 psig and 80 psig are introduced, respectively. This trend is similar to what was seen for the case of $2^{nd}$ order model case.

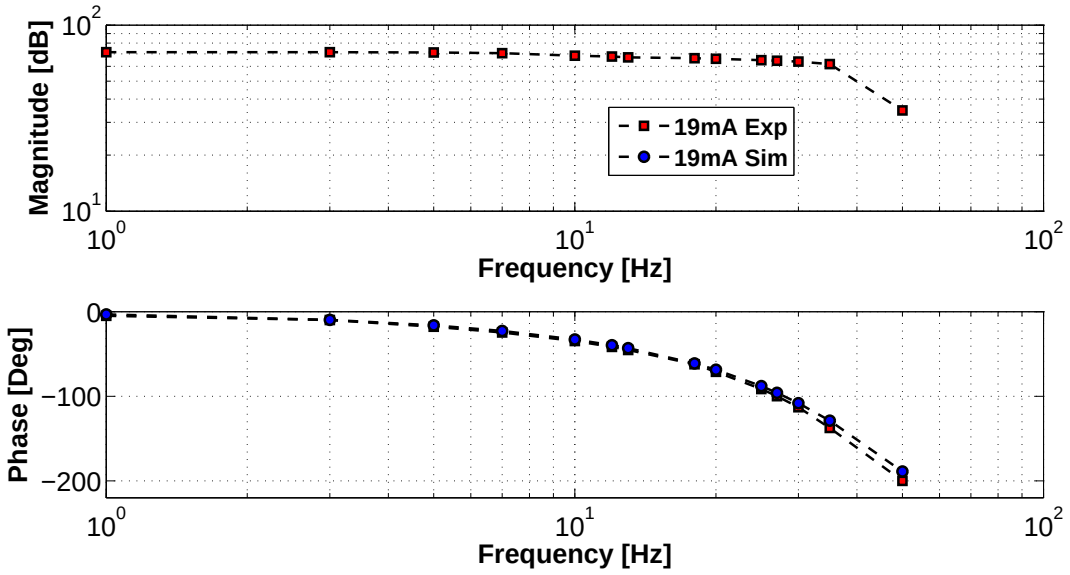


Figure 3.8: $4^{th}$ order non- parametric model.

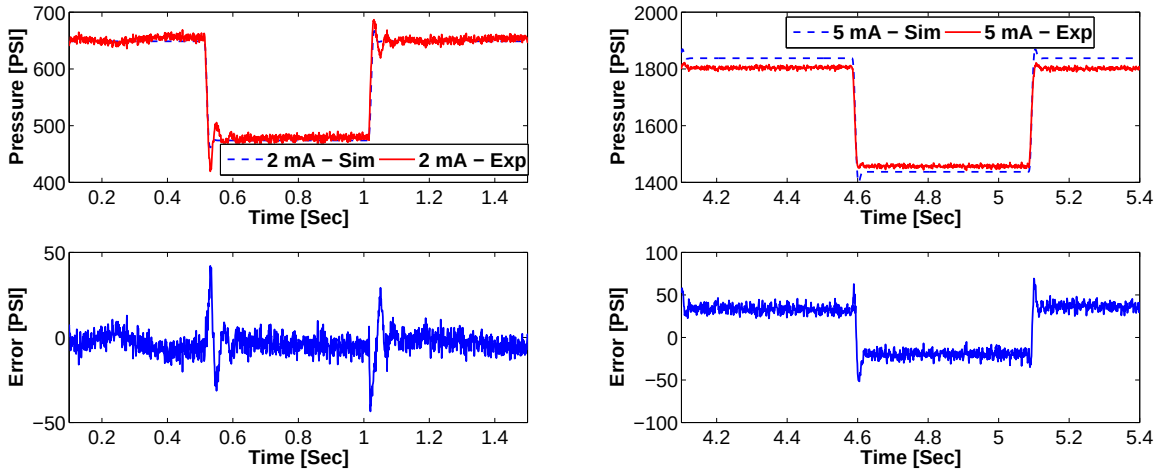


(a) 2mA control current step input.

(b) 5mA control current step input.

Figure 3.9: $4^{th}$ order model fit simulation results

### 3.3.5 $2^{nd}$ and $4^{th}$ order model comparison

In order to compare the performance of both the models, $2^{nd}$ order and $4^{th}$ order, Figure 3.10 shows their unit step response and Table 3.2 shows the rise time, settling time and peak of each model. It is clear that the $2^{nd}$ order model settle and rises faster and has a lower overshoot compared to the $4^{th}$ order model. Even though the specifications of the

Table 3.2: $2^{nd}$ and $4^{th}$ order model specifications

| $2^{nd}$ **order** | | $4^{th}$ **order** | |
|---|---|---|---|
| **Rise Time (sec)** | 0.0064 | **Rise Time (sec)** | 0.0086 |
| **Settling Time (sec)** | 0.0177 | **Settling Time (sec)** | 0.0269 |
| **Peak** | 1.0433 | **Peak** | 1.088 |

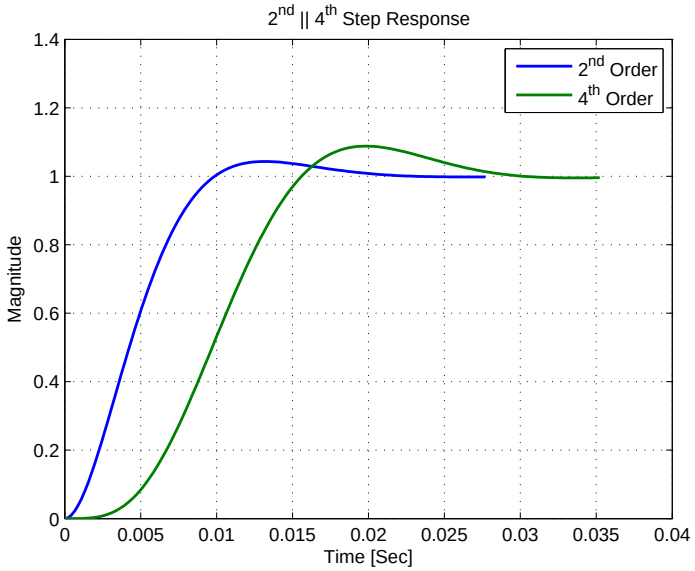


Figure 3.10: Unit Step Response $2^{nd}$ and $4^{th}$ order model

$4^{th}$ order model look worse compared to the $2^{nd}$ order model, Figure 3.11 really justifies why the $4^{th}$ order model represents the BCV better. It is easy to see that the Least Square

Estimation (LSE) can not be used because the system is not a 1st order system. However, the results of the simulation for the $4^{th}$ order system have improved 3 times compared to the $2^{nd}$ order system. For a control current command with a step of 5 mA the error is 210 psig and 70 psig for $2^{nd}$ and $4^{th}$ order system, respectively. Thus, even when the specifications of the $4^{th}$ order system are not as impressive as the $2^{nd}$ order system, the $4^{th}$ order system imitates the Brake Control Valve (BCV) more closely.

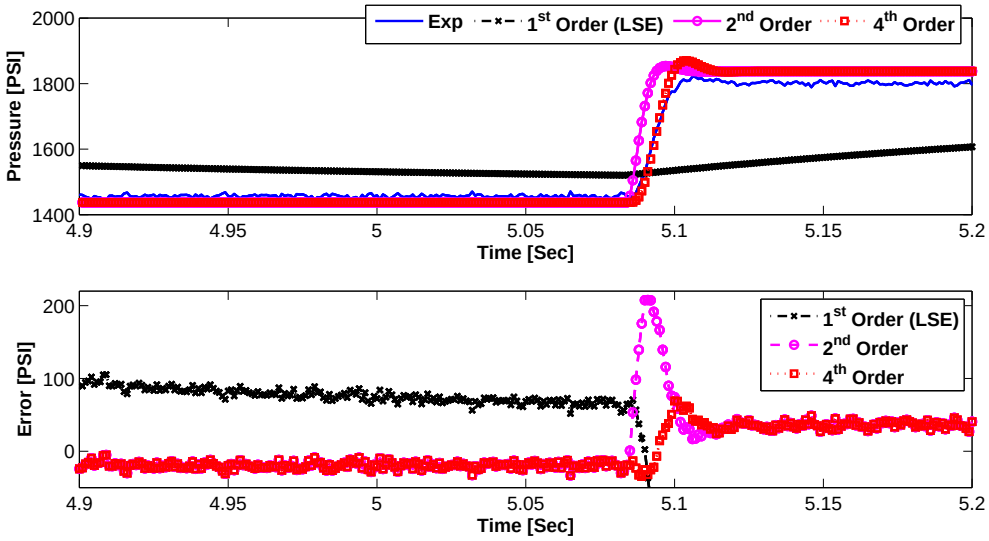


Figure 3.11: $2^{nd}$ and $4^{th}$ order model Simulation results

## 3.4 Controlling the BCV

Once the Brake Control Valve is established in a system as shown in Figure 3.12(a), in order to regulate the pressure generated by the Brake Control Valve (BCV) and control its behaviour, the control strategy shown in Figure 3.12(b) is employed. The BCS is made of two main components: the antiskid braking system (ABS) block and the brake by wire (BBW) block. The BBW block produces the control signal to the current driver for the BCV while the ABS block helps regulate the control signal to avoid the wheel slip. When

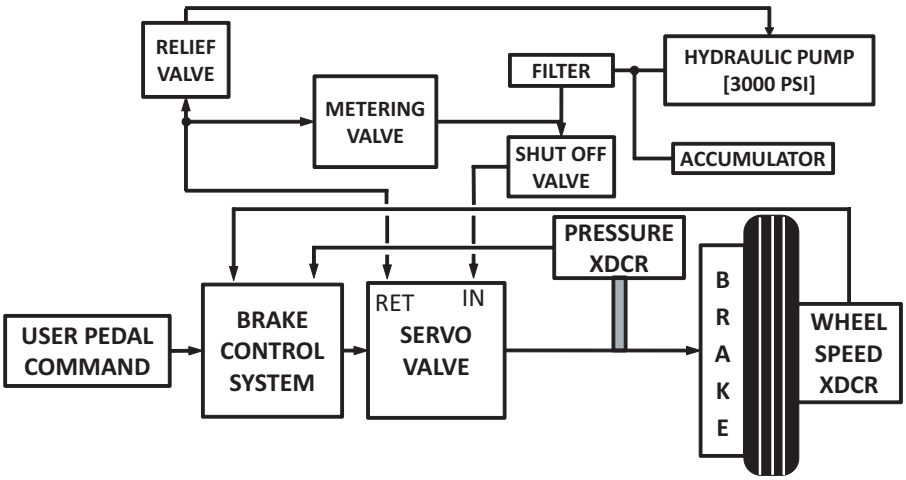


(a) Block diagram of the BCS connected with the brake hydraulic circuit.

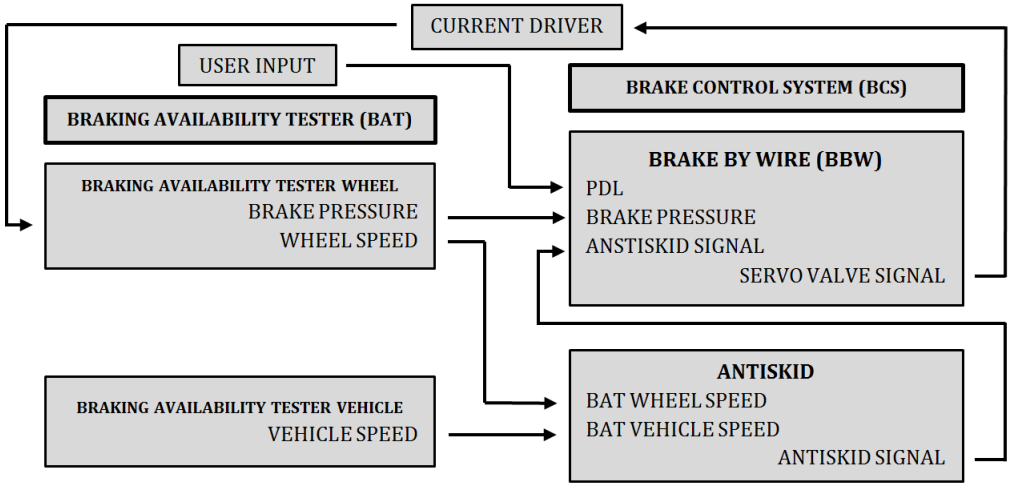


(b) Brake Control System (BCS).

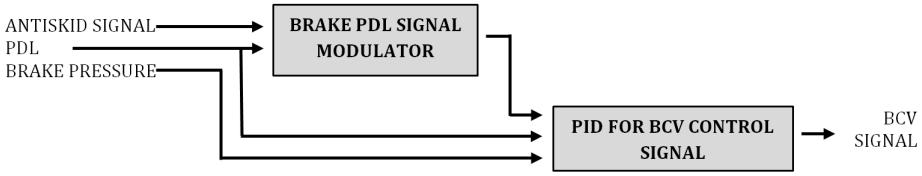


(c) Brake by Wire (BBW).

Figure 3.12: Overview of the BCS

BAT wheel starts to skid, the BCS sends a control current command to the BCV which causes the flapper to move resulting in a lower pressure at the biased end of the slide. This increases flow from the BRAKE port to the RETURN port and decreases the brake pressure to the brake caliper (See Figure 3.1(b)). Brake Control System (BCS) keeps lowering this pressure until it notices that the BAT wheel is not skidding. Once this is achieved, BCS starts to increase the brake pressure at the brake calipers again and repeats the process until the vehicle decelerates at the required rate. The BCS continually adjusts braking to runway conditions, during which the BCV flapper and slide move continuously by adjusting the control current to the servo part of the BCV.

### 3.4.1 Brake Control System (BCS)

The ABS controller implemented in the BAT is built upon the commercial algorithm from *Meggit Aircraft Braking Systems Corp.*, a leading aircraft braking system supplier. The actual algorithm has been simplified and modified to achieve braking performance similar to that of Boeing 737 by accounting for the scale factor and the operation mode of the BAT. Currently, a single ABS algorithm is used for proof-of-concept but the BCS will eventually consist of a number of different ABS algorithms for different types of aircrafts. The runway tests will be conducted by cycling all the available ABS algorithms. BCS can be broken down to two main components: brake by wire (BBW) and Antiskid. BBW produces the control signal to the current driver for the BCV while the antiskid block helps regulate that signal such that the BAT wheel operates under fully functional aircraft ABS. The overall structure of the BAT working with the BCS is shown in Figure 3.12(b).

### 3.4.2 Brake by Wire (BBW)

Brake by wire contains the feedback loop that controls the command that is sent to the BCV current driver by combining the antiskid signal and the pedal signal provided by the BAT operator. Also, the brake pressure read by the pressure transducer at the brake calipers is used as an important feedback signal. The brake pedal modulator continuously observes the current state of the BAT wheel due to the application of the brakes by the

operator as seen in Figure 3.12(c). The PID loop acts as a strict regulator in order to control the brake pressure. Brake pressure feedback signal is filtered with a 50 Hz low pass filter to remove excessive noise for better application of the PID controller (See Figure 3.13) with Proportional $(K_p)$, Derivative $(K_d)$ and Integral $(K_i)$ gains calculated with the help of the BCV model developed. Moreover, there is a bias current provided to the BCV to overcome the back pressure at the brake pads.

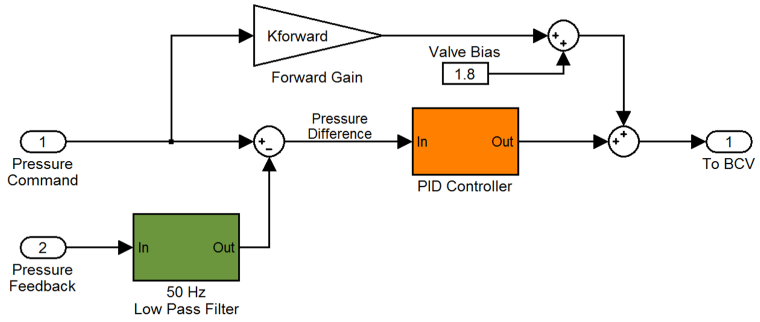


Figure 3.13: PID for BCV Control Signal.

### 3.4.3 Antiskid

Antiskid provides safety against skidding of the BAT wheel while applying enough brake pressure to generate required drag force for different road conditions. It takes into consideration the speed of the BAT vehicle and the BAT wheel to provide the antiskid signal that can be used to generate the BCV signal to the current driver as seen in Figure **??**. BCS found in the BAT is much different compared to the conventional ABS found in automobiles since it is the BCS of a Boeing 737 aircraft. The BCS used in the BAT can control the brake pressure in order to control the deceleration rate of the BAT vehicle. Since the BAT vehicle decelerates only by applying braking at the BAT wheel, not a high rate of deceleration for the BAT vehicle can be achieved. This is mainly due to the mass of the BAT vehicle. The Antiskid continuously monitors the speed of the BAT wheel in order to detect sudden changes for controlling the deceleration rate and the braking pressure.

# Chapter 4

# Braking Availability Quantification

The approach taken by the BAT to quantify the braking availability is distinct from that in current practice which typically goes as follows. The conventional friction device first provides a representative value. Due to the inconsistency and uncertainty of the value on heavily contaminated runways, various contributing factors are then taken into account such as the type and depth of contaminants, the speed of the test vehicle, wheel load of the test vehicle, pavement texture, tire tread depth, etc. The effects of these factors are applied by either empirical or theoretical models. The Paved Runway Condition Assessment Table developed through TALPA/ARC represents one of major efforts to standardize the effect of contaminant types and depths for non-wet and not-dry runways. Although such efforts have improved the predictability of braking performance on contaminated runways, there still exist potential issues [14]. It is unclear how many contributing factors one should consider. Besides, the effect of one factor may vary with other factors. Therefore, we consider such a model-based approach has a fundamental limitation.

The approach taken by the BAT can be considered as the data-driven approach. Instead of focusing on the effect of component factors, the BAT focuses more on the comprehensive (or aggregate) effect i.e. the progression of the drag force as a result of contributing factors (whichever they are). In order for such a data-driven approach to be meaningful, the device should be able to replicate the braking conditions of the target aircraft as closely as possible, which led to the design concept of the BAT. In this chapter, we briefly introduce

an analytical method that can be used to quantify the braking distance of landing aircraft using the measurement data acquired by the BAT. The method proposed in this section is aimed at finding not the  value but the velocity-dependent drag force profile.

### BAT Data-Driven Approach

The horizontal drag (or resistance) being applied to a landing aircraft can be represented as

$$F_h = F_f + F_a \tag{4.1}$$

where $F_f$ is the frictional drag due to tire-pavement interaction that can be measured by the horizontal load cell and $F_a$ is the aerodynamic drag. $F_f$ can be further broken up into two components

$$F_f = F_{br} + F_r \tag{4.2}$$

where $F_{br}$ is the braking resistance and $F_r$ denotes the rolling drag. The BAT is primarily designed for estimating the combined effect of $F_{br}$ and $F_r$ (i.e. $F_f$). In stationary case where we assume constant friction and uniform road, $F_{br}$ and $F_r$ can be described as functions of the vertical load:

$$F_{br} = \mu N, \quad F_r = \frac{b}{r} N \tag{4.3}$$

where $N$ is the normal force applied to the tire, $\mu$ is the friction coefficient, $b$ is the rolling resistance coefficient, and $r$ is the wheel radius [15], as shown in Figure 4.1. Equation (4.3) is the model behind the existing runway condition monitoring systems, which presumes that the braking availability can be quantified by a single constant $\mu$ (a friction coefficient). Experimental results using B737 and BAC 1-11 [16] show that $F_{br}$ as well as $F_r$ is far from constant on wet and contaminated runways. Another important fact on contaminated runway is that, water and slush increase the rolling drag of a tire due to displacement of the water/slush. This is in contrast to a dry runway where the rolling drag $F_r$ is almost negligible compared to $F_{br}$. Although there have been some attempts to analytically predict the rolling drag due to snow compaction [17], it is generally not possible to do so for composite contaminants mixed with snow, slush and water.

As explained in the previous section, the main concept of the BAT is to mimic not only the brake hardware but also the brake controller of the actual aircraft. For example, an

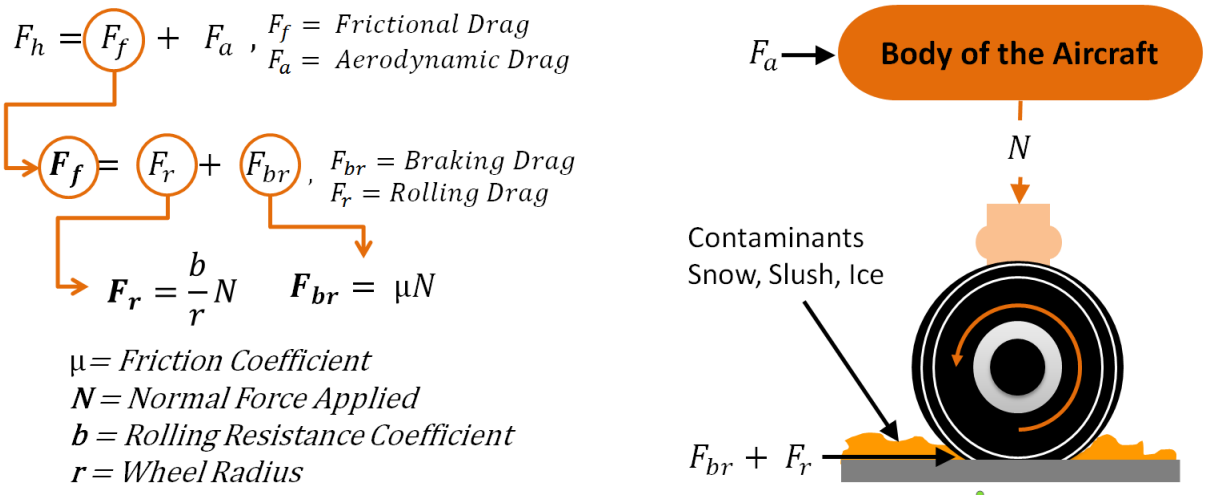


Figure 4.1: Friction forces acting on an aircraft.

On-Off type BCS would effectively use only about 70% of the available friction on a dry surface, and less on a contaminated surface. A modern, modulating type of BCS is designed to use at least 90% of the available friction even on a very wet surface. Most of modern airplanes are equipped with ABS yet none of the existing runway friction devices operates under the ABS, which may cause a significant error from the actual braking availability of landing airplane on contaminated winter runways [18]. Therefore, the incorporation of the ABS has been identified as a differentiating factor in designing the BAT. Previous data in [16] indicate that the frictional characteristics such as the $\mu$ and the contamination drag significantly varies with velocity (and thus with time) under the effects of deformable contaminants and the operation of the ABS. This suggests that we should treat the frictional drag $F_f$ as a function of vehicle velocity, i.e., $F_f = F_f(v(t))$ where $v(t)$ denotes the speed of the vehicle (or the aircraft being braked). The BAT can run in various speeds up to 120 km/h. To authors' knowledge, this is wider than the speed range that most of existing devices can operate. More importantly, the BAT can reveal the effect of varying slip ratio due to change of speed unlike most of existing devices that run on a fixed slip ratio.

The BAT can be operated in various ways to extract useful information on the braking availability of the runway. One possible procedure is to run the BAT at various speeds.

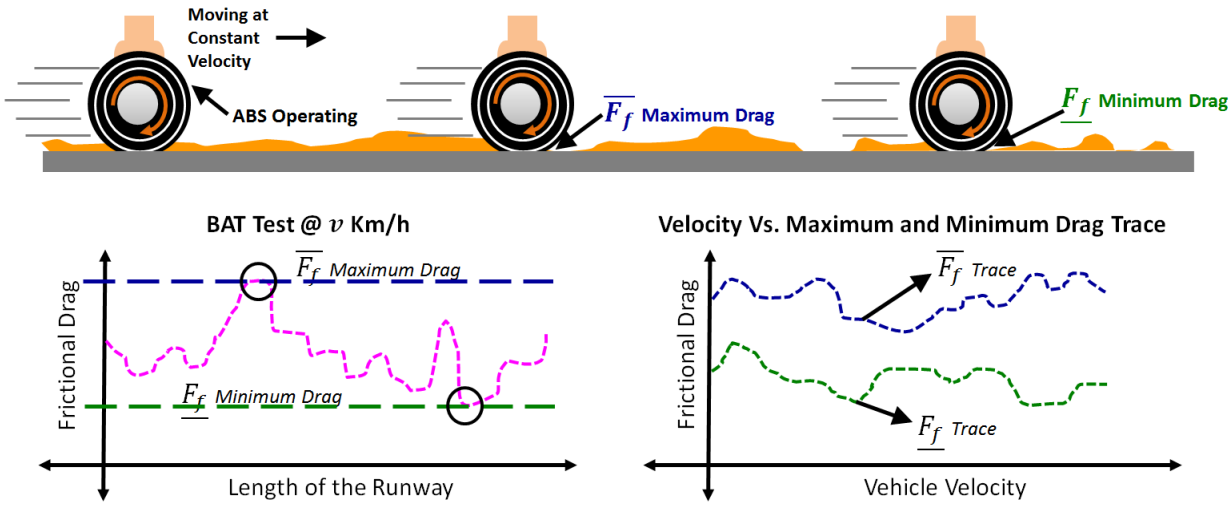


Figure 4.2: Testing and data collection.

For example, we can run the BAT with its speed at a constant value for a short period of time (2∼3 seconds) and repeat it at other speeds. Running the BAT in this way will provide us with the mapping between $v$ and $F_f$ as shown in Figure 4.2.

By Newton's law, the vehicle speed can be related to the (time-varying) drag force as follows.

$$F_f(v(t)) = -m\frac{dv(t)}{dt} \tag{4.4}$$

where $m$ denotes the inertia of the vehicle. The total time for the vehicle to stop, say, $t_s$ can then be written as

$$t_s = -m\int_{v(0)}^{v(t_s)} \frac{1}{F_f(v)}dv = m\int_0^{v(0)} \frac{1}{F_f(v)}dv. \tag{4.5}$$

where we used the fact that $v(t_s) = 0$.

Then, the velocity and position of the BAT at the stop time $t = t_s$ can be represented as

$$x(t_s) = x(0) + t_s v(0) - \int_0^{t_s}\int_0^{t} \frac{F_f(\tau)}{m}d\tau dt \tag{4.6a}$$

$$v(t_s) = v(0) - \int_0^{t_s} \frac{F_f(\tau)}{m}d\tau \tag{4.6b}$$

Thus, $x(t_s)$ projects the total stopping distance to be expected based on the BAT test data.

In the above analysis, we have assumed that the mapping between $v$ and $F_f$ is static. In reality, the horizontal drag is not necessarily constant for a constant velocity (See Figure 4.2). This may come from the non-uniform distribution of the deformable contaminants or the runway condition over the stretch of the runway. As a result, the horizontal drag will be represented by a range

$$\underline{F}_f(v(t)) \leq F_f(v(t)) \leq \overline{F}_f(v(t)) \tag{4.7}$$

where the underbar and the overbar notation indicate the minimum and maximum values of $F_f$, respectively for the corresponding vehicle speed. Replacing $F_f$ in Eqs. (4.5),(4.6a) and (4.6b) by $\underline{F}_f(v(t))$ or $\overline{F}_f(v(t))$ will provide us with the maximum or the minimum braking availability, respectively for the current runway condition being tested. The measured horizontal drag is not for an aircraft but for the BAT. Therefore, in order to relate this value to an actual aircraft, various correction factors can be considered as shown in 4.8.

$$F_f^{ac}(v_\ell^{ac}(t)) = C_{tire} \cdot C_{mass} \cdot C_{cor} \cdot F_f(C_{vel} \cdot v(t)) \tag{4.8}$$

where the superscript "$ac$" denotes the corresponding variable for a certain aircraft model (e.g. Boeing 737). $C_{tire}$, $C_{mass}$, $C_{vel}$ and $C_{cor}$ represent correction factors to account for additional effects coming from the differences in the tire (e.g. pressure or footprint), the total mass, the touchdown speed and any other correlation factor, respectively.

The analysis in the above only involves the drag due to tire-pavement interaction. The ultimate index for the braking availability as well as the correction factors in Eq. (4.8) will be devised in combination with the flight data. During the winter time in the coming years, the BAT will go through extensive field tests at the Region of Waterloo International Airport in collaboration with WestJet Airlines. The correlation with the flight data will be investigated accordingly.

# Chapter 5

# Experimental Tests for ABS operation and Frictional Drag Measurement

The use of actual aircraft ABS is one of the main features of the BAT. To verify the operation of the BCS and other functionalities of the BAT, we conducted road tests on the asphalt pavement surface (the regional road 5 Line W in Campbellford, Ontario). The road test has been conducted in two different weather conditions: dry road and snowy road. Some parameters for the road test are listed in Table 5.1. The testing procedure

Table 5.1: Conditions for BAT road test

| Parameter | Value | Unit |
|---|---|---|
| Vertical load to the BAT wheel (N) | 1000 | [kg] |
| Vehicle speed before brake application | 80 | [km/h] |
| Time duration of brake application | $5 \sim 8$ | [sec] |
| Hydraulic system pressure | 3000 | [psi] |
| Maximum braking pressure | 1850 | [psi] |
| Tire rolling radius ($R_{eff}$) | 22.1 | [cm] |

is as follows. While the BAT truck remains stationary, the BAT wheel is lowered down, during which the 1,000 kg of vertical loading is applied by the vertical cylinder (See Figure 2.2). Then, the truck is accelerated to 80 km/h, after which the brake force is applied with a constant brake pressure. During the brake application, the transmission gear of the truck has been put to neutral position so as to allow the truck to slow down. To simulate the brake operation used in airplanes, the brake command is applied through the brake pedal simulator where the maximum desired brake force is set by the percentage of maximum braking pressure. Considering 1,000 kg of the vertical load, 1,850 psi of brake pressure has been selected as the maximum allowable brake pressure.

## 5.1 Test on Dry Pavement

The dry road test has been conducted in the morning of November 27th 2012. Figure 5.1 shows the road surface at the time of testing.

Figure 5.1: The test road under a dry weather condition.

The braking performance has been monitored with different percentages of brake pedal command: 30%, 45%, 70% and 100%. The corresponding drag forces measured by the horizontal load cell are shown in Figure 5.2. The drag force signal is relatively uniform

and constant except for the 100% one where the ABS becomes active. It is clear that the maximum braking occurs around 70% of brake pedal since the 100% pedal provides a similar drag force to the 70% pedal.

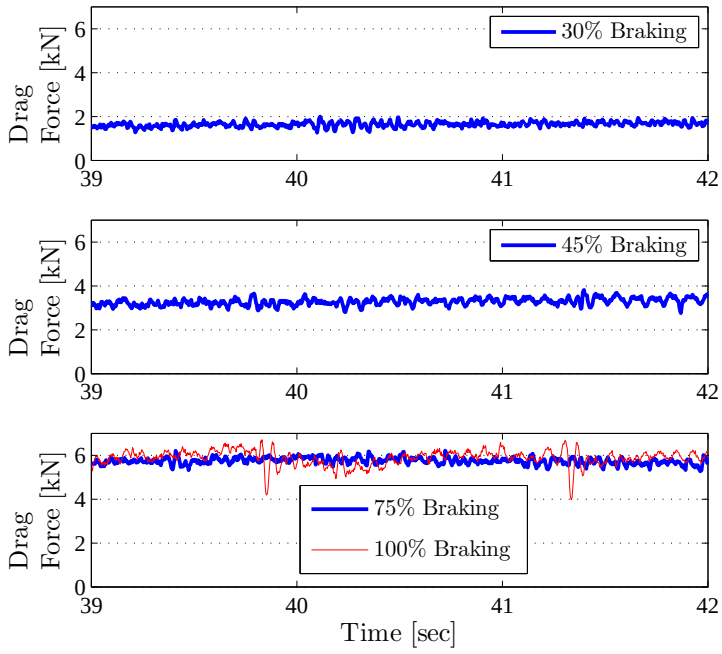


Figure 5.2: Drag force measured by the horizontal load cell for different values of brake pedal command on a dry pavement.

Figures 5.3 and 5.4 show the original data for the 45% pedal and the 100% pedal, respectively. The subplot (a) in each figure shows the actual brake pressure measured by pressure transducer. The brake pressure in Figure 5.3(a) is close to the target value (i.e., 960 psi) commanded by the pedal. On the other hand, the brake pressure in Figure 5.4(a) is much smaller than the target pressure (1,850 psi). This is because the ABS does not allow the brake pressure to rise high enough to cause any skidding. Note that the fluctuation in the brake pressure of Figure 5.4(a) also demonstrates that the ABS operates in such a way that it instantly modulates the brake pressure whenever needed to prevent the BAT wheel from skidding.

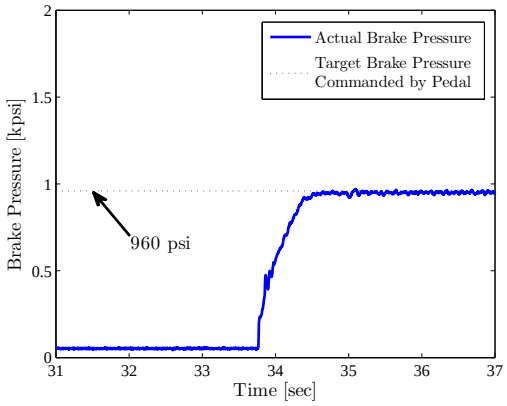


(a) Brake pressure.

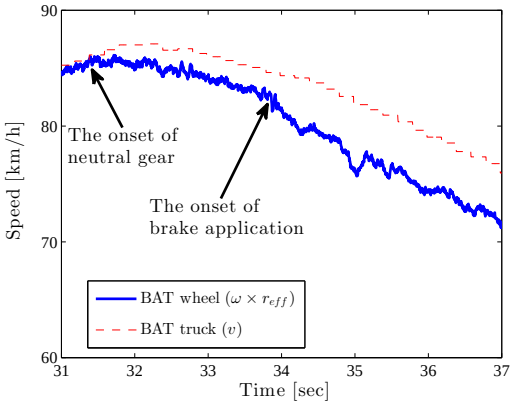


(b) Speeds of the BAT and the vehicle.

Figure 5.3: Braking performance for 45% pedal. (The ABS is not active.)

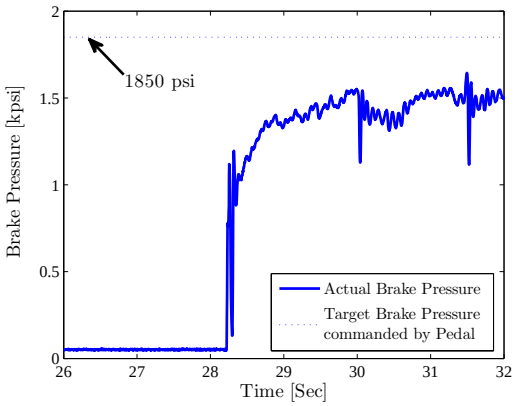


(a) Brake pressure.

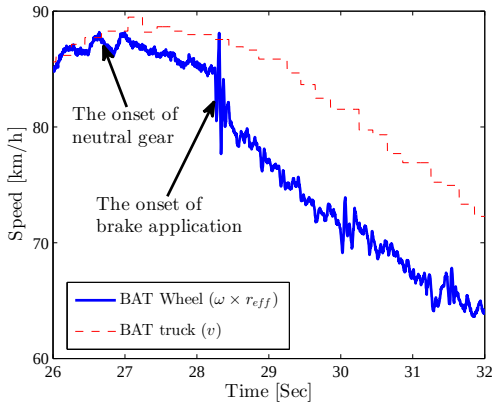


(b) Speeds of the BAT and the vehicle.

Figure 5.4: Braking performance for 100% pedal. (The ABS becomes active.)

The subplot (b) in Figures 5.3 and 5.4 show how the BAT wheel and the BAT truck decelerate during the same time interval as that of the plot (a). The thin dashed line represent the BAT truck speed measured by the GPS and the thick solid line indicates the product of the BAT wheel speed ($\omega$) and the rolling radius ($r_{eff}$). As defined through Eq. (5.1), the difference between these two lines represent the corresponding slip ratio $\sigma$. As mentioned in the test procedure, the transmission of the truck has been put to neutral before the brake pedal is commanded. The corresponding time instants for the neutral gear and the brake application are indicated by the black arrows in respective plots. As we can see in Figures 5.3 and 5.4, a certain amount of slip occurs as soon as the gear is put to neutral, and it subsequently increases when the brake is applied. The amount of slip before the onset of the brake represents the rolling drag $F_r$ (See Eq. (4.2)). Figure 5.4(b) also shows that the BAT truck decelerates faster with the 100% braking than the 45% one. Another important observation from Figure 5.4 is that the sudden drops of the brake pressure at $t = 30$ s and $t = 31.6$ s in Figure 5.4(a) are due to the rapid drops of the BAT wheel speed shown in Figure 5.4(b) which occurred at the same time instants. During this process, the ABS maintains the maximum possible brake force without any wheel slip, which demonstrates the performance of the ABS.

Figure 5.5 shows the relation between the slip ratio ($\sigma$) and the friction drag force ($F_f$). The slip ratio for braking is computed using the BAT wheel speed $\omega$, the tire rolling radius $r_{eff}$ and the vehicle speed $v$, i.e.

$$\sigma = \frac{v - \omega \cdot r_{eff}}{v}. \tag{5.1}$$

The circle marks denote the data obtained from the experiment. The percentage value for each data point represents the corresponding brake pedal command. As we can see, the maximum braking occurs between 70% and 100% and the ABS has been active on these two data points. The interpolation curve is obtained by using the Pacejka model for typical tire-pavement friction characteristics [19].

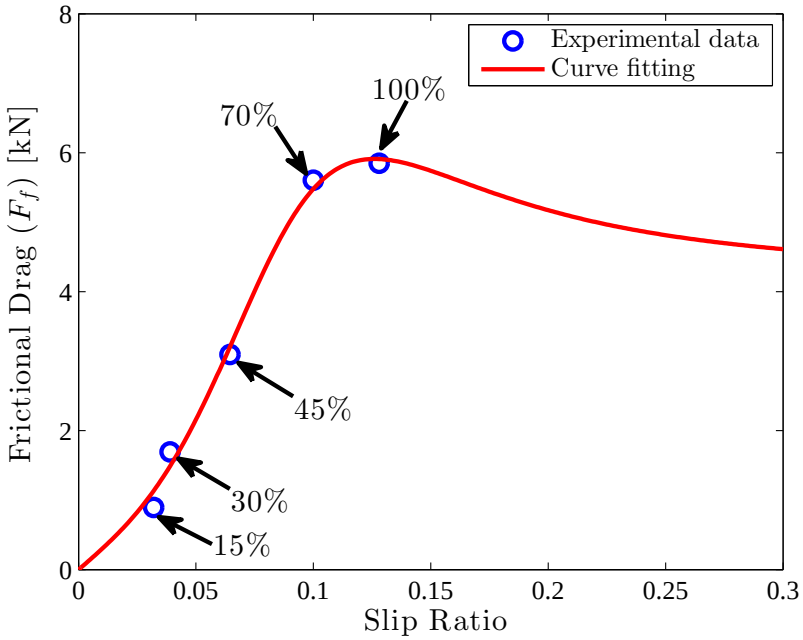


Figure 5.5: Tire-pavement frictional characteristics on a dry pavement.

## 5.2 Test on Contaminated Pavement

The dry road test demonstrated the baseline performance of the BCS to simulate normal braking behavior for different brake pedal commands. It also verified the performance of the instrumentation system that monitors in situ the status of the BCS and the tire-pavement interaction.

To validate the performance of the BAT on contaminated pavement, additional tests have been performed on snowy road.

The second experiment was conducted around 6:30 am EST (Eastern Standard Time) on March 19th 2013 when the test road is covered by about 2 to 3 cm of fresh snow. Figure 5.6 shows the road surface at the time of testing. Due to the slippery pavement, the test was performed at speeds ranging from 60 to 70 km/h which are a little lower than those used in the dry road test.

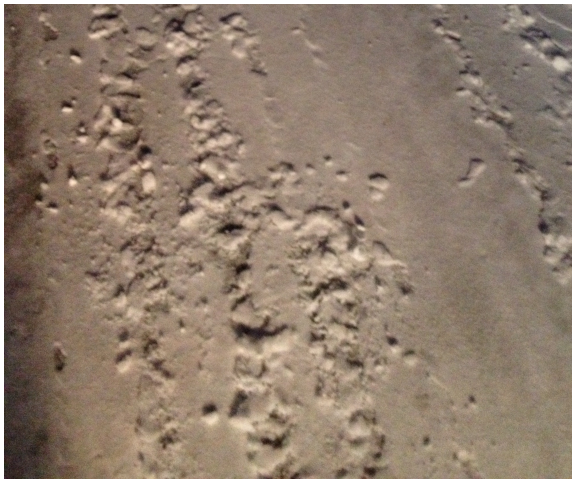

Figure 5.6: The test road covered by snow.

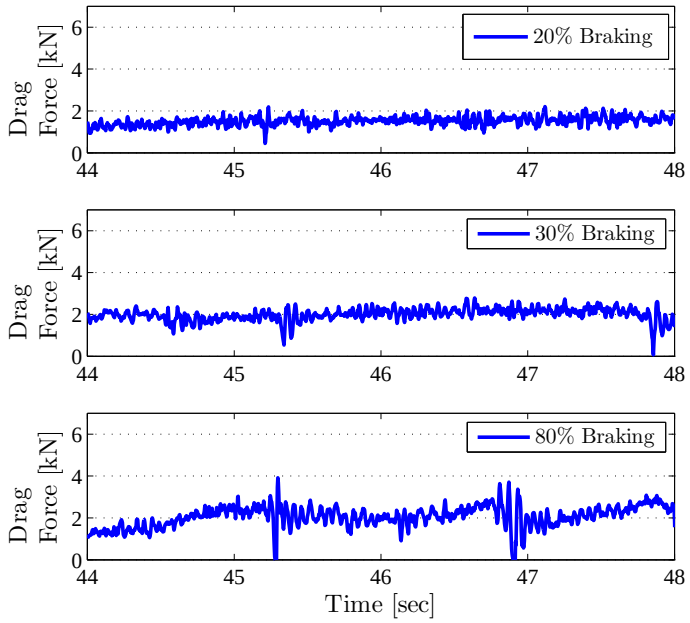


Figure 5.7: Drag force measured by the horizontal load cell for different values of brake pedal command when the test road is covered by snow.

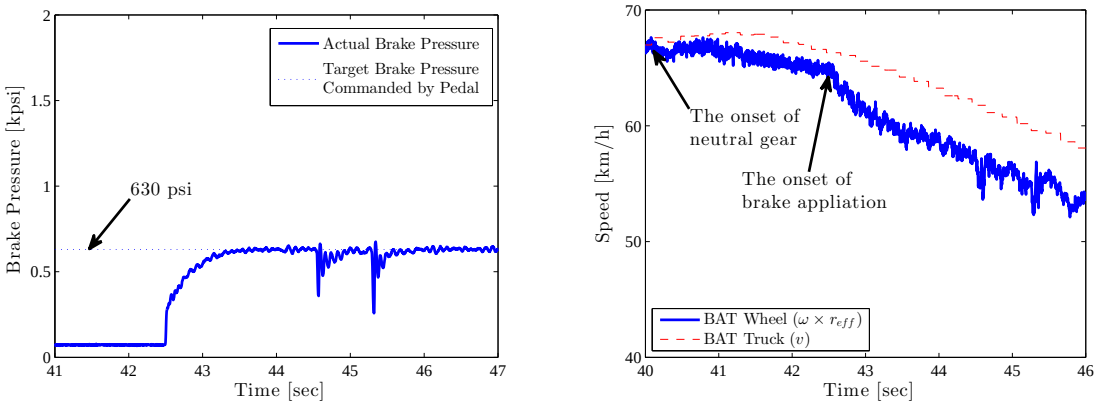


(a) Brake pressure.

(b) Speeds of the BAT and the vehicle.

Figure 5.8: Braking performance for 30% pedal. (The ABS is not active.)

The first observation is that the drag force signals do not rise above 2 kN even for high brake pedal command (See Figure 5.7). Besides, most of the drag force signals reveal more fluctuating behavior than those from the dry road test shown in Figure 5.2, which implies that the ABS become active at much lower percentage ($\sim 30\%$) of brake pedal command.

Figures 5.8 through 5.10 show the original data for 30%, 45% and 100% pedal command, respectively. Figure 5.8(a) shows that a small amount of modulation occurs due to intermittent slippage of the wheel although the brake pressure is mostly catching up with the desired value. However, for higher brake pedal commands shown in Figures 5.9(a) and 5.10(a), the brake pressure profiles keep fluctuating almost randomly without maintaining any constant pressure at any time interval. It is clear that the braking behavior on highly contaminated pavement is fundamentally different from that on the dry pavement due to the operation of the ABS. Such a transient behavior in the brake pressure is well reflected in the speed profiles in Figures 5.9(b) and 5.10(b) where the BAT wheel intensely alternates between rolling and slipping. The subplot (b) in Figures 5.8 through 5.10 is drawn with the same scale so that we can see how the deceleration of the BAT truck differs from each other. Since the braking capability is dominated by the ABS and not by the commanded brake pressure, the resultant deceleration is very similar in all three cases of pedal commands.

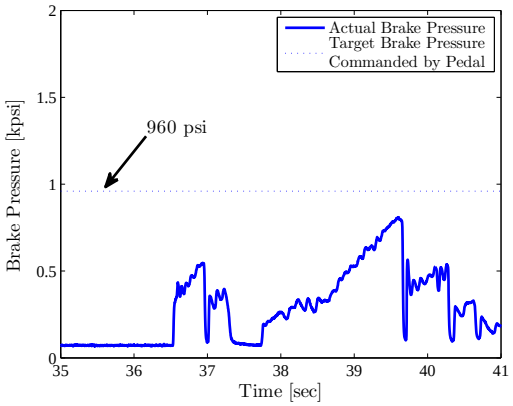


(a) Brake pressure.

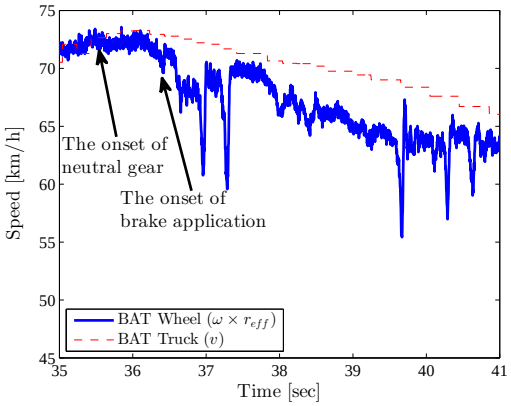


(b) Speeds of the BAT and the vehicle.

Figure 5.9: Braking performance for 45% pedal. (The ABS is active.)

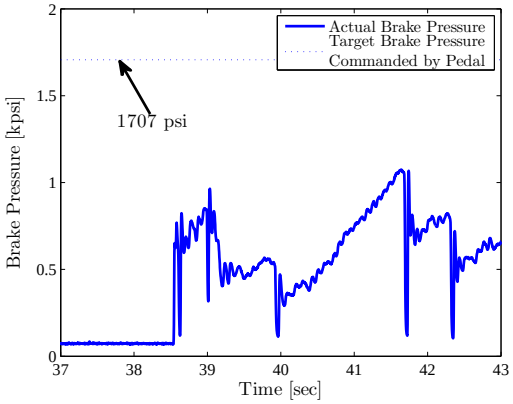


(a) Brake pressure.

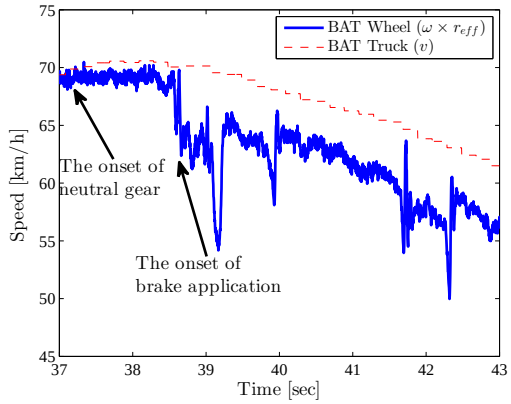


(b) Speeds of the BAT and the vehicle.

Figure 5.10: Braking performance for 80% pedal. (The ABS is active.)

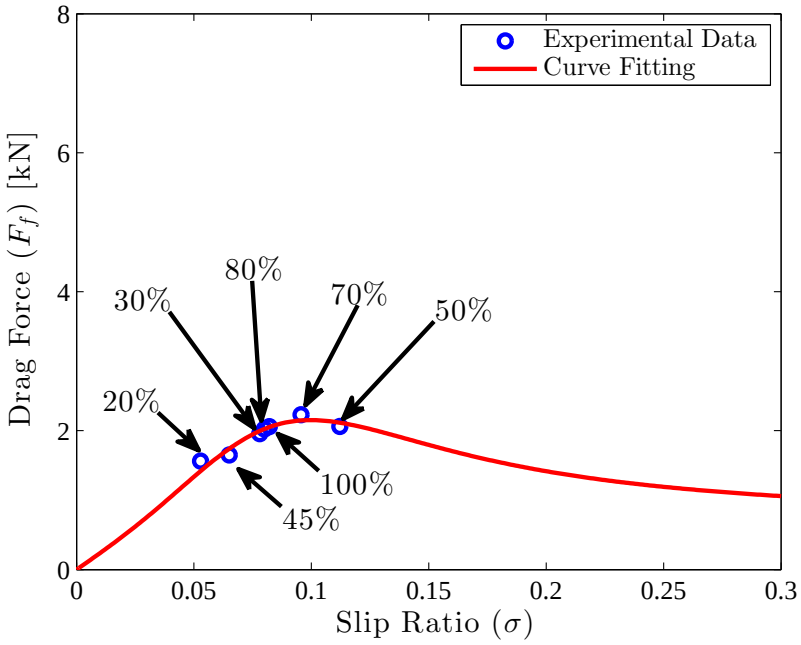


Figure 5.11: Tire-pavement frictional characteristics on test road covered by snow.

The experimental results presented here clearly suggest that the conventional way of identifying the braking capability may not represent the actual braking behavior on snowy pavement under the operation of the ABS. It is still possible to approximate such a transient braking behavior with a constant $\mu$ value (e.g. by averaging). Figure 5.11 shows the corresponding $\mu$-slip curve using the "averaged" drag force and slip ratio on snow pavement. Again, the circle marks are the averaged data points and the solid line is the curve fitting with the Pacejka model. Note that the slip ratio and drag force do not show a trend as consistent as that in Figure 5.5. The sample points are rather randomly scattered between 30% braking and 100% braking with their slip ratio widely varying from 5.5% to 11.5%. Such an inconsistent behavior is somewhat expected from the brake pressure and wheel speed profiles shown in Figures 5.8 through 5.10.

# Chapter 6

# Concluding Remarks

## 6.1 Conclusion

The aviation industry has long been in need of more realistic assessment of braking availability for landing airplanes. This has been especially true for winter runways where the deformable contaminants and constantly changing weather conditions make it a challenge to reasonably predict the landing distance. To overcome the limitations of existing technologies, the BAT is developed based on the idea of mimicking the braking performance of an actual aircraft. As a result, the brake control system, the brake hardware and the landing gear mechanism similar to those of actual aircrafts have been realized by the BAT. This thesis has elaborated on the design concept and operational principles and all the other parts that make up the device. The brake control system appears to be operating as expected on a dry or damp surface.

Additionally, the BAT can be used to predict the condition of the runway under various weather condition to help improve pilot's judgement. Data-driven approach taken by the BAT can provide realistic results for the immediate condition of the runway. This can be used to estimate the safe landing distance required for the aircraft. The experimental results from the dry and contaminated surfaces prove that the BAT is functional and operational for further testing.

## 6.2 Future Work

In partnership with Region of Waterloo International Airport and Westjet Inc., the BAT field testing has officially been launched on March 27th 2013. The measurement data from the BAT, the pilot data from the Westjet aircrafts and the runway monitoring data from the Region of Waterloo International Airport will be correlated and collectively analyzed to realize a new braking availability index.

Sensor accuracy and inconsistency has limited results from the BAT testing that has been done at this time. The sensors, instrumentation, and the structure needs to be upgraded to improve the quality of the results. Moreover, a self-wetting system is being worked on to simulate contaminated runway at the BAT wheel. This will make BAT testing less dependent on the weather conditions. The antiskid control may require some adjustment for operating in very wet environment. It should be possible to make some tuning adjustment with the current system.

In parallel with the correlation effort using the BAT, the research team at the FAA has been conducting a similar test with an actual aircraft. The collaborative research agreement has recently been established between the BAT team and the FAA to share the knowledge developed by each party in the next few years.

# References


[1] F. S. Foundation, Aviation safety network, Online (April 2013).

[2] R. S. Initiative, Reducing the risk of runway excursions, Technical report, Flight Safety Foundation (May 2009).

[3] X. Junchi, Overview of certification of aeroplane takeoff and landing performance on contaminated runways, Procedia Engineering 17 (2011) 13–23.

[4] A. K.-P. A. B. H. J. D. A. P. G. H. J. B. T.-B. Langedahl, Braking performance of commercial airplanes during operation on winter contaminated runways, Cold Regions Science and Technology 79-80 (2012) 29–37.

[5] Y. Jiang, Review on flight performance certification standard for wet and contaminated runway, Procedia Engineering 17 (2011) 7–12.

[6] N. T. S. Board, World airways, inc., flight 30h,boston-logan international airport, ntsb/aar-85/06, Aviation accident report, United States Government, Washington, D.C. (September 1985).

[7] N. T. S. Board, Southwest airline flight 1248, chicago midway international airport, ntsb/aar-07/06, Aviation accident report, United States Government, Washington, D.C. (October 2007).

[8] N. T. S. Board, Pinnacle airlines flight 4712, cherry capital airport, ntsb/aar-08/02, Aviation accident report, United States Government, Washington, D.C. (June 2008).

[9] N. T. S. Board, Large airplane operations on contaminated runways, Technical report, United States Government, Washington, D.C. (April 1983).

[10] E. A. S. Agency, Certification specifications for large aeroplanes cs-25, Technical report, European Aviation Safety Agency (September 2008).

[11] C. G. W. H. Astrom, Friction measurement methods and the correlation between road friction and traffic safety, Technical report, Swedish National Road and Transport Reasearch Institute, Linkoping, Sweden (2001).

[12] N. T. S. Board, Safety recommendation a-07-58 through -64, Technical report, Federal Avaition Administration, Washington, D.C. (October 2007).

[13] Sensing, C. H. Inc., Model RGF - Rod End In-line Compression/Tension Load Cell, 1985 Douglas Drive North Golden Valley, MN 55422 www.honeywell.com, 2010.

[14] E. A. S. A. (EASA), Workshop runway friction and aircraft braking: The way forward, Technical report, Paris, France (2001).

[15] H. R, Engineering Mechanics: Statics and Dynamics., Pearson, Prentice Hall 11th Edition, 2007.

[16] N. A. Laboratory, Safety aspects of aircraft performance on wet and contaminated runways, report no. nlr - tp - 2001 - 216, Technical report, Amsterdam, Netherlands (2001).

[17] G. van Es, Model for predicting the rolling resistance of aircraft tires in dry snow, Journal of Aircraft 36 (1999) 762–768.

[18] V. Battista, Performance of abs-equipped vehicles on deformable surfaces.

[19] R. Rajamani, Vehicle Dynamics and Control, Springer, New York, 2006.

[20] F. S. Service, Safo 06012, landing performance assessments at time of arrival (turbojets), Technical report, Federal Aviation Industry, Washington, D.C. (August 2006).

[21] N. I. Incorporation, National Instruments Devices/Modules, Austin, Texas, 2013.

[22] C. Aerospace, I. Electronics, Hydro-Aire, Component maintenance manual with illustrated parts list, brake control valve 39-815, Technical report, Burbank, CA (September 2009).

[23] H. Inc., GTN1A111 Series Hall-Effect Gear-Tooth Sensor for heavy duty applications, 50 Clarke S Woodstock, ON N4S 8Y7, 2013.

[24] Sauer-Danfoss, MBS1250 Heavy Duty Pressure Transmitter, 300 Airport Rd. Ames, IA 50011 USA, 2009.

[25] A.-T. I. Ltd., Series LWG - Position Transducers up to 750 mm, Toronto, ON Tel: 416-754-7008 Fax: 416-754-2351, 2008.